

University of New Mexico

UNM Digital Repository

Earth and Planetary Sciences ETDs

Electronic Theses and Dissertations

Fall 11-15-2021

The Birth and Incision History of the San Juan River in the Past 5 Ma

Micael T. Albonico

Follow this and additional works at: https://digitalrepository.unm.edu/eps_etds



Part of the [Geology Commons](#)

Recommended Citation

Albonico, Micael T.. "The Birth and Incision History of the San Juan River in the Past 5 Ma." (2021).
https://digitalrepository.unm.edu/eps_etds/321

This Thesis is brought to you for free and open access by the Electronic Theses and Dissertations at UNM Digital Repository. It has been accepted for inclusion in Earth and Planetary Sciences ETDs by an authorized administrator of UNM Digital Repository. For more information, please contact disc@unm.edu.

Micael Tomas Albonico

Candidate

Earth and Planetary Sciences

Department

This thesis is approved, and it is acceptable in quality and form for publication:

Approved by the Thesis Committee:

Karl E. Karlstrom , Chairperson

Laura J. Crossey

Mary L. Gillam

Matthew T. Heizler

**THE BIRTH AND INCISION HISTORY OF THE SAN JUAN
RIVER IN THE PAST 5 MA**

by

MICAEL T. ALBONICO

B.S., GEOLOGY, NORTHERN ARIZONA UNIVERSITY 2014

THESIS

Submitted in Partial Fulfillment of the
Requirements for the Degree of

Master of Science in Earth and Planetary Sciences

The University of New Mexico
Albuquerque, New Mexico

December, 2021

ACKNOWLEDGEMENTS

I thank National Science Foundation awards EAR-1348007 [to Dr. Karl Karlstrom], and EAR-1545986 [to Dr. Laura Crossey and Dr. Karl Karlstrom], for partial support. I thank Grand Canyon National Park for research and collecting permits (to Dr. Karl Karlstrom and Dr. Laura Crossey). I thank UNM alumni and the NMGS grants-in aid program for partial support.

I would like to thank my adviser Dr. Karl Karlstrom for his guidance and enthusiasm in this project. I would also like to thank my committee members, Dr. Laura Crossey for her academic and financial support; Dr. Mary Gillam for her constant geologic advisement and field insights in the Animas Valley; Dr. Matthew Heizler and the members of the New Mexico Geochronology Research Laboratory in Socorro, NM for their technical expertise with $^{40}\text{Ar}/^{39}\text{Ar}$ analyses; Dr. Andres Aslan from Colorado Mesa University for his expertise and insights.

Additionally, I would like to thank my wife Colleen and my family members for their constant support throughout my academic career.

THE BIRTH AND INCISION HISTORY OF THE SAN JUAN RIVER IN THE PAST 5 MA

By

Micael Albonico

B.S., Geology, Northern Arizona University, 2014

M.S., Earth and Planetary Sciences, University of New Mexico, 2021

ABSTRACT

This study addresses the evolution of the San Juan River system and its confluence with the Colorado River, ~ 100 km above the regionally important Lees Ferry knickzone. The San Juan River is a 600-km-long continental-scale tributary of the Colorado River. From its headwaters in the San Juan Mountains in Colorado, the San Juan River flows across the Colorado Plateau, and into the Colorado River upstream of Grand Canyon. Published apatite fission track and apatite (U-Th)/He thermochronologic data show that rocks in Marble Canyon, as well as in middle and upper reaches of the San Juan River, were >75 °C and hence buried by 1.5-2 km of overlying strata until rapid cooling after ~5 Ma. This ~5 Ma age marks the birth of the San Juan system and its integration with the Colorado River as we know it. The longitudinal profile of the San Juan River is generally concave-up, with no major knickpoints. This apparent “equilibrium” river profile contrasts with the Colorado and Little Colorado rivers that have major bedrock-influenced knickzones coincident with the Kaibab Limestone. This paper evaluates incision rates through time across the Lees Ferry knickzone and in the lower, middle, and upper reaches of the San Juan River to evaluate alternative models for river evolution. Incision rates are constrained using new $^{40}\text{Ar}/^{39}\text{Ar}$ detrital sanidine (DS) dating of river terraces. We dated over 5000 grains, from 27 terraces, yielding ~ 2% young (< 2 Ma) grains that give

important new maximum depositional ages (MDAs) and minimum incision rates for 18 of the terraces. The most common youngest grains were ca. 0.63, 1.2, and 1.6 Ma and, in most reaches, the terraces containing 0.63 Ma grains are ~half as high above the river as the terraces containing 1.2 Ma grains suggesting steady average incision over the past 1.2 Ma. However, age-correlative terraces are very different heights and yield different incision rates reach to reach: 143-160 m/Ma for eastern Grand Canyon and Marble Canyon, 219-270 m/Ma along the Colorado River in Glen Canyon above Lees Ferry knickzone, 97-128 m/Ma in the San Juan River as it crosses the Colorado Plateau, and up to 237 m/Ma in the San Juan Mountain headwaters. Steady incision argues against punctuated climatic events or transient knickpoint migration in the past 1.2 Ma and suggests differential uplift. Adding to the previously proposed ~150 m/Ma surface uplift of eastern Grand Canyon relative to the Gulf of California based on downstream differential incision, our differential incision magnitudes imply an additional 100 m/Ma uplift of paleoriver profiles across the broad, ~200-km-wide, Lees Ferry knickzone and ~100 m/Ma uplift of the San Juan Mountains headwaters relative to the Colorado Plateau. If incision has been steady over 5 Ma, with thermochronologic data inferring more rapid exhumation in the 5-2 Ma timeframe after integration, this suggests that the Lees Ferry knickzone region is the edge of the uplifting southwestern Colorado Plateau region that has given rise to Grand Canyon, and that the San Juan Mountains region has simultaneously been uplifted ~ 500 m relative to the Colorado Plateau over the past 5 Ma. The rate changes are spatially associated with sharp mantle velocity transitions and we infer that they reflect mantle-driven differential epeirogenic uplift.

TABLE OF CONTENTS

LIST OF FIGURES X

LIST OF TABLESXii

INTRODUCTION.....1

 Previous river incision studies on the Colorado Plateau.....5

 Thermochronology constraints on regional denudation9

METHODS 11

 Single crystal ⁴⁰Ar/³⁹Ar dating of detrital sanidines in river terraces 11

RESULTS 13

 Terrace characterization..... 13

 Eastern Grand Canyon 14

 Marble Canyon..... 15

 Glen Canyon 17

 San Juan- Colorado River confluence..... 18

 Colorado River above San Juan-Colorado River confluence 19

 San Juan River above Colorado River confluence 20

 Animas River/ Upper San Juan River..... 21

Detrital sanidine results.....	23
Eastern Grand Canyon	26
Marble Canyon.....	27
Glen Canyon	27
San Juan- Colorado River confluence.....	28
Above San Juan-Colorado River confluence to Bullfrog Marina.....	28
Mexican Hat to Farmington	29
Animas River/ Upper San Juan River.....	29
INTERPRETATION AND DISCUSSION.....	30
Interpretation of maximum depositional ages.....	30
Comparison of different age dating methods for river terraces	31
Terrace correlation using detrital sanidine provenance and age.....	33
Climatic influences on terrace development.....	35
Paleoprofile synthesis	37
Alternative models for the Lees Ferry knickzone.....	41
Evaluating mantle-driven uplift	46
CONCLUSIONS	51
DATA REPOSITORY	53

List of data repository materials	53
Data tables	54
DR Table 1	54
Photos of dated terraces	55
P-25	55
P-7	55
P-24 and P-32	56
P-14	56
P-26	57
P-18	57
SJR-2	58
A-4.....	58
A-6.....	59
Bullfrog Terrace	59
REFERENCES CITED.....	60

LIST OF FIGURES

Figure 1. Regional map of study area.	2
Figure 2. Nested river profiles of the San Juan River with physiographic features, 5 Ma thermochronology-derived paleosurface, and generalized geologic cross section from the Little Colorado confluence to the San Juan Mountains.....	3
Figure 3. Terrace correlation from previous workers showing new and compiled dated terraces.....	14
Figure 4. Modified terrace maps and dated samples for upper Marble Canyon of the Colorado River.	16
Figure 5. Terrace maps and dated samples for Glen Canyon of the Colorado River, above Glen Canyon Dam and below the San Juan River confluence.....	18
Figure 6. Stacked high terraces in Oak Bay near the Colorado-San Juan River confluence..	19
Figure 7. Terraces photos and locations at Bluff and Mexican Hat, Utah and at Bullfrog Marina on the Colorado River.....	21
Figure 8. Animas River Valley terrace map and longitudinal profile.....	22
Figure 9. Summary of 0 – 40 Ma detrital sanidine grains from the study area.	25
Figure 10. Relative probability plots and $^{40}\text{Ar}/^{39}\text{Ar}$ analysis of youngest grain populations and schematic illustration of recycled grains in Glen Canyon (high incision area).	26
Figure 11. Pleistocene felsic caldera eruptions in western North America and $^{40}\text{Ar}/^{39}\text{Ar}$ relative probability plots of the 1.23 Ma lower Bandelier Tuff.	35

Figure 12. Colorado and San Juan River pre-dam river profiles showing terraces heights and locations and the inferred 1.2 Ma and 0.6 Ma paleoprofiles. 40

Figure 13. Alternative hypotheses for the Lees Ferry knickzone 42

Figure 14. Compiled average long-term incision rate data, P-wave velocity, tomographic cross section, and nested longitudinal profiles of the Colorado River and its major tributaries plotted from the Gulf of California to the Colorado Rocky Mountains; river distance in kilometers. 48

Figure 15. Simplified longitudinal profiles of the Colorado River system and schematic drawing of differential uplift interpretation across the Colorado Plateau..... 50

LIST OF TABLES

TABLE 1. RIVER TERRACES DATED WITH DETRITAL SANDINE IN THIS STUDY

.....23

INTRODUCTION

The San Juan River is a major tributary of the Colorado River that flows from >4-km elevations of the southern Rocky Mountains through an impressive landscape of bedrock canyons and slot canyons within the interior of the Colorado Plateau. The river changes character from a mountain stream in its headwaters in the San Juan Mountains of southwestern Colorado to a wider river across the Colorado Plateau through Farmington, New Mexico and Bluff, Utah, and eventually flows into the Colorado River at Glen Canyon, ~ 80 km north of Lees Ferry in the area now flooded by Lake Powell (Figure 1).

Figure 2 shows the river's longitudinal elevation profile in the context of landscape features projected in from around it. The headwater tributaries of the San Juan River, including the Animas River discussed here, drain a rugged complex of Precambrian crystalline basement, Paleozoic and Mesozoic sedimentary rocks, and Tertiary volcanic rocks of the San Juan Mountains that have high peaks reaching above 4000 m (Figure 2; Cross and Larson, 1935). Transitioning from the San Juan Mountains to the northern San Juan Basin, Figure 1 shows that most of the northern headwater tributaries (Mancos River, La Plata River, Animas River, Los Pinos River, Piedra River, and Navajo River) flow down the slopes of the San Juan Mountains and Hogback monocline. The southern tributaries join the San Juan River in the synclinal zone of the Hogback monocline (Chaco River) and Monument monocline uplift (Chinle Creek). West of the Monument uplift, the San Juan River carves deep sinuous bedrock canyons with entrenched meanders, including the Goosenecks area west of Mexican Hat, Utah. The San Juan River finally flows into Glen Canyon and meets the Colorado River in the area now covered by Lake Powell. Accurate pre-dam estimates of the elevation of the confluence and profiles of the San Juan and Colorado rivers in Figure 2

are from Birdseye et al. (1922).

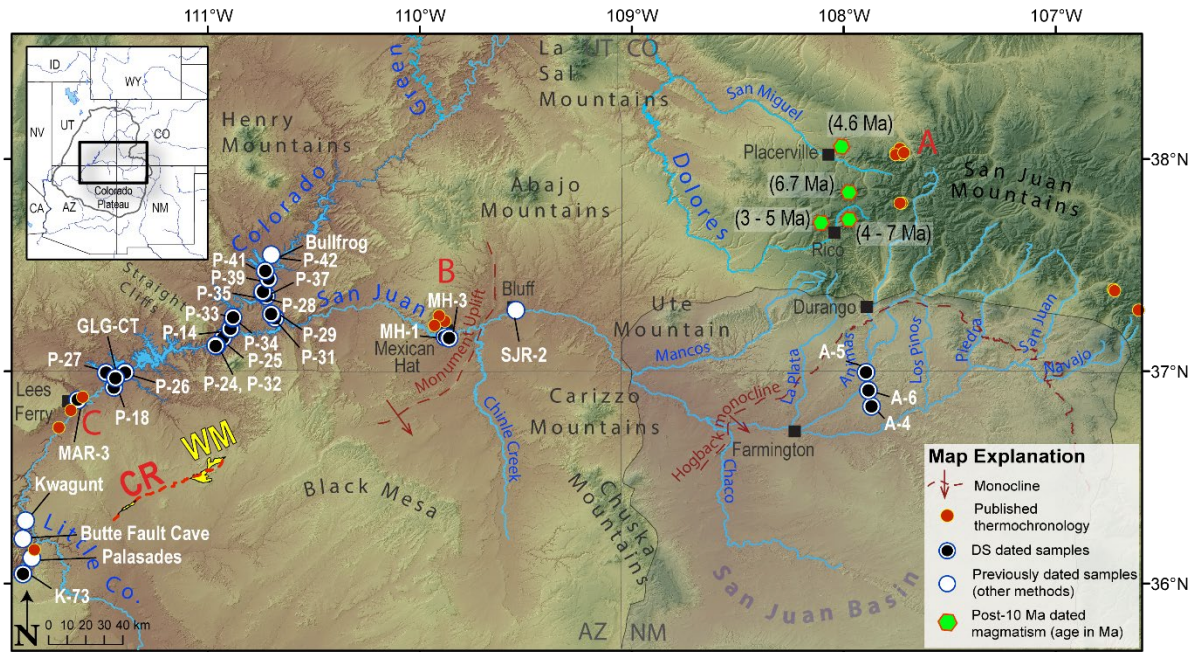


Figure 1 - Regional map of the San Juan River drainage and its major tributaries spanning the four corners of Colorado, New Mexico, Utah and Arizona. The red circles indicate thermochronology samples collected in: A) the headwaters of the San Juan River in the San Juan Mountains, north of Durango (McKeon, 2009; Kelley and Karlstrom, 2017); B) near the middle drainage of the San Juan River by the Monument upwarp (Hoffman, 2009); and C) below Lake Powell at Lee’s Ferry (Lee et al., 2012) and near the Little Colorado River confluence (Karlstrom et al., 2014). The white and black circles indicate incision control points for the San Juan River in the upper drainage on the Animas River (Gillam, 1998), the middle drainage near Bluff, Utah (Wolkowinsky and Granger, 2004; Heizler et al., 2021), and the lower drainage above and below the confluence of the San Juan - Colorado River in Bullfrog, UT (Darling et al., 2012) and below Lees Ferry at Kwagunt and Palasades near river mile 56 and 65 of the Colorado River (Crow et al., 2014). Green hexagons in the western San Juan Mountains near Rico and Placerville, Colorado, are locations of young (7 – 4 Ma) magmatism (Gonzales, 2015; 2017).

Other nearby landscape features shown in Figure 2 that help pose the research questions about landscape evolution of the Colorado Plateau and incision history of the San Juan River system include: Black Mesa and Straight Cliffs, held up by upper Cretaceous sandstones; Ute, Carrizo and Navajo mountain laccoliths of Laramide age that bow-up Cretaceous strata (Condie, 1964; Gonzales, 2015); the Abajo and La Sal mountain laccoliths

of 29 Ma (Rønnevik et al., 2017), and paleosurfaces in the Chuska Mountains of 35 and 27 Ma below and above the Chuska Sandstone (Cather et al., 2008). Generalized geology and height of canyon rims along the San Juan and Colorado rivers are shown by the thin red line in Figure 2. The goal of this paper is to investigate the incision history of the San Juan River system through time since its integration with the Colorado River at about 5 Ma.

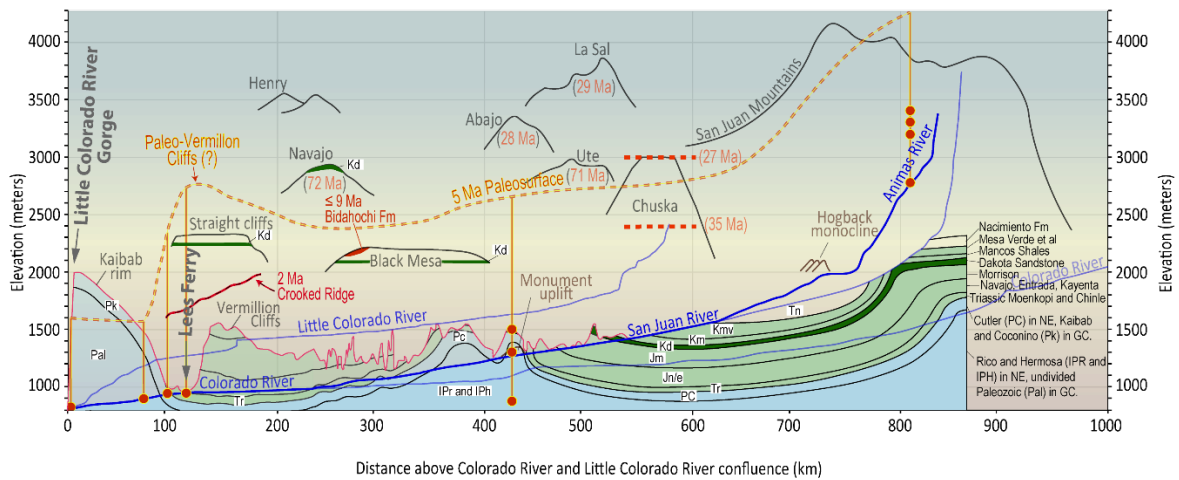


Figure 2 - Nested river profiles of the San Juan River (thick, dark blue line) from lower reaches in the San Juan-Colorado River confluence to upper reaches in the San Juan Mountains, Colorado, and Little Colorado Rivers. Cross section of major geologic units hung along the profile of San Juan River, with steep entrenched canyons shown by the thin red line. Physiographic features and “sky islands” are presented to show the relative landscape traversed by the San Juan River. The yellow dashed line shows the approximate 5 Ma paleosurface reconstructed, using thermochronology data in the Lower (Lee et al., 2012; Karlstrom et al., 2017), middle (Hoffman, 2009), and upper (McKeon, 2009; Kelley and Karlstrom, 2017) reaches, assuming a geothermal gradient of 25 °C/km and a surface temperature of 15 °C. The 35 Ma and 27 Ma Chuska erosion surfaces are indicated by the thick red dashed lines (Cather et al., 2008).

An estimated 5 Ma paleosurface that pre-dates integration of the Colorado River through Grand Canyon is reconstructed in Figure 2 based on apatite thermochronologic studies. These data suggest that rocks along the entire length of the San Juan River underwent rapid cooling after 5 Ma due to erosional removal of ~2 km of strata (Hoffman,

2009; Mckeon, 2009; Karlstrom et al., 2012; Lee et al., 2012; Kelley and Karlstrom, 2017). This suggests that the San Juan River has been integrated with the Colorado River and in its present location only since 5 Ma. An older, perhaps Oligocene/Miocene, San Juan paleoriver was proposed by previous workers to be preserved in the Crooked Ridge/ White Mesa alluvium gravels (Figures 1 and 2; Babenroth and Strahler, 1945; Strahler, 1948; Cooley and Davidson, 1963; McKee et al., 1967; Hunt, 1969; Lucchitta et al., 2011; 2013; Lucchitta and Holm, 2020) but these fluvial deposits have now been dated with detrital sanidine as < 2 Ma and, based on the age, high landscape position, and steep gradient of the Crooked Ridge system, it has been reinterpreted as younger tributary gravels to the paleo Little Colorado River (Hereford et al., 2016; Karlstrom et al., 2017; Heizler et al., 2021). Thus, the existence and location of any pre-5 Ma paleo San Juan River pathway across the region at stratigraphic positions within Cretaceous rocks higher than the yellow line paleosurface in Figure 2 remain speculative and are not recorded by any preserved deposits or landscape features.

We apply new detrital sanidine $^{40}\text{Ar}/^{39}\text{Ar}$ dating to terrace flights along the San Juan and Colorado river system from Grand Canyon to the San Juan Mountains. These terraces extend back 1-2 Ma (Wolkowinski and Granger, 2004) and preserve a long-term record of the river's incision history. This San Juan River transect is an important test bed for the concept that differential river incision can be a proxy for differential uplift, and specifically that the Rocky Mountains have been uplifting relative to the Colorado Plateau over the past 10 Ma (Karlstrom et al., 2012) at the same time that the Colorado Plateau has been uplifting relative to the Gulf of California (Karlstrom et al., 2008; 2012; Crow et al., 2014; Crow et al., 2019). The broader motivation of this study is to test models for young and potentially ongoing mantle-driven epeirogenic surface uplift of the Rocky Mountain region.

Previous river incision studies on the Colorado Plateau

Some river incision studies have proposed semi-steady incision through time in a given reach, and varying rates in different regions, and explained these in terms of tectonic elements such as faulting or mantle velocity transitions that may imply differential regional uplift across the Colorado Plateau and the Colorado Rocky Mountain regions (Karlstrom et al., 2012). Studies of the Colorado River (Karlstrom et al., 2008; Crow et al., 2014) and its tributaries of the Virgin (Walk et al., 2019) and Little Colorado rivers (Karlstrom et al., 2017) support ~1 km of surface uplift of the Colorado Plateau relative to the river's baselevel at the Gulf of California since the Colorado River first flowed into the Gulf of California between 4.8 and 4.63 Ma (Crow et al., 2021). In this hypothesis, the Lees Ferry knickpoint at the head of Grand Canyon marks a major change between the steep lower basin profile through Grand Canyon that is responding to the lower base level, and lower gradients of the Colorado Plateau that may not have seen the base level change (Darling et al., 2012).

Some studies have reported higher incision rates above the Lees Ferry knickpoint than below (Garvin et al., 2005; Cook et al., 2009; Pederson et al., 2013). These higher rates were measured over shorter (~ 100 ka) timescales and could reflect real increases in youngest incision rates in the past 100 ka due to glacial-interglacial oscillations (Aslan et al., 2019). Alternatively, they may reflect application of different dating methods where, for example, terrace tread ages from cosmogenic surface dating are minima compared to longer-term bedrock incision measured by strath ages as constrained by other methods (Karlstrom et al., 2013). This uncertainty highlights the present limitations of incision rate studies for which there are: 1) relatively few well-dated long-term incision rate localities where average

incision rates can be measured for timescales of 0.3 to 2 Ma; 2) even fewer areas where multiple terrace heights in a given reach can be used to test steady versus non-steady strath-to-strath bedrock rates at the million-year time frame, and 3) few rivers where rates-through-time data can be compared from one reach to another along their length. A major goal of this study is to provide new incision data points and strath-to-strath rates through time at numerous locations near the confluence of the San Juan and Colorado rivers that can be compared to the relatively well studied Grand Canyon incision rate data (e.g., Crow et al., 2014) and thereby improve the understanding of incision history across the Lees Ferry knickzone.

Differential river incision studies on the western (Rosenburg et al., 2014) and eastern (Nereson et al., 2013) flanks of the Colorado Rocky Mountains have also suggested up to ~ 1 km of surface uplift of the Rockies relative to the Colorado Plateau in the past 10 Ma. Rosenburg et al. (2014) analyzed several rivers that crossed from the Rocky Mountains to the Colorado Plateau: Little Snake, Yampa, White, and upper Colorado Rivers. Incision magnitudes along these sub-parallel west-flowing rivers increased from north to south, from ~550 m to ~1500 m over the past 10 Ma with higher normalized channel steepness, higher incision magnitudes, and higher incision rates corresponding to regions underlain by low velocity upper mantle. These studies found steady incision at the million-year timescale in a given reach coupled with different, but still steady, rates in other reaches.

Reconciling long-term, intermediate-term, and short-term timescales over which incision rates are measured is important to deciphering the forces influencing incision. As reported by Aslan et al. (2019) for the Upper Colorado River system, short-term (<100 ka)

incision rates vary widely (~250 - 750 m/Ma) which probably reflects the unsteady nature of glacial/ interglacial climate-influenced incision. Intermediate-term (100 ka to 1 Ma) incision rates range from ~200 - 300 m/Ma, and long-term (> 1 Ma) incision rates average ~110 - 160 m/Ma. Aslan et al. (2019) reported 1513 m of total incision since the time of deposition of the first known Colorado River deposits below the 10.81 Ma Grand Mesa basalt yielding a long-term average incision rate of 140 m/Ma. There are acknowledged uncertainties in whether incision was steady in some reaches (e.g. Glenwood Canyon at 110 m/Ma), but Aslan et al. (2019) generally supported the tectonic differential uplift hypothesis. Lazear et al. (2013) and Aslan et al. (2019) argued that the long-term pace of incision is not completely accounted for by isostatic rebound resulting from exhumation. Erosional isostasy can explain between 500-800 m of post-10 Ma uplift, about half of the total reported 800-1700 m of post-10 Ma river incision and rock uplift in the upper Colorado River Basin (Lazear et al., 2013). The other ~half (500-1000 m) of the observed fluvial incision and rock uplift may best be explained by tectonic forcings that triggered differential erosion and related rebound.

In some cases, incision rate changes take place across zones of transition in mantle velocity suggesting that upper mantle flow and sharp buoyancy changes at 60-100 km depths between low mantle velocity domains and high velocity domains may be driving young and ongoing differential uplift. Roy et al. (2009) and Crow et al. (2011) documented a migration of increasingly young and more asthenospheric basaltic volcanism toward the Colorado Plateau center that is compatible with this model for deep-seated mechanisms driving regional epeirogenic uplift. This leads to the hypothesis that long-term steady incision at different rates in different parts of a continental-scale river system may be the signal of mantle driven epeirogenic differential uplift in the Rocky Mountain-Colorado Plateau region.

The Colorado River first reached the Gulf of California about 5 Ma (5.33 according to Dorsey et al., 2007; refined to 4.8-4.63 Ma by Crow et al., 2021), and the Colorado River profile has been graded to sea level since about 4.6 Ma (Crow et al., 2021). Thus, similar to Walk et al. (2019), the regional river system provides a “laboratory” to conduct this differential incision analysis progressively upstream from sea level at the Gulf of California and to add up differential uplift amounts relative to the sea to quantify surface uplift over the past 5 Ma.

The San Juan River system is ideally suited to continue to test the Rocky Mountain uplift part of this hypothesis because it crosses from the Colorado Plateau to high elevations of the San Juan Rocky Mountains and is tied to the Colorado River at their confluence ~ 100 km above the Lees Ferry Kaibab Limestone knickpoint. The goal of this study is to date terrace flights using detrital sanidine to evaluate steady versus non-steady incision over the past few million years and evaluate any variations across the Lees Ferry knickpoint and across the transition from the Colorado Plateau to the Rocky Mountains. Terrace targets for this study include: 1) the highest terraces in eastern Grand Canyon, 2) terrace flights just above the Lees Ferry knickpoint that include ~ 8 terrace levels that extend from 140–330 m above the pre-Dam river level (Billingsley and Priest, 2013); 3) terraces above and below the San Juan-Colorado confluence in Lake Powell (Glen Canyon) that extend from 100 m to 370 m above the pre-dam river level (Garvin et al., 2005); 4) terraces near Mexican Hat and Bluff, Utah that extend from 80 m to 150 m above river level (Wolkoinsky and Granger, 2004); 5) terraces near Farmington, New Mexico that extend from 70 m to 130 m above the river; and 6) terraces along the upper San Juan in the Animas River drainage that extend > 200 m above the rivers, including a terrace near the middle of the terrace flight that is directly

dated by the 630 ka Lava Creek B ash (Gillam, 1998). Some of these terraces that had been previously dated by other methods such as U-series dating of carbonate, cosmogenic surface dating of terrace treads, and cosmogenic burial dating of gravels allow comparison of these results with the new detrital sanidine data.

Thermochronology constraints on regional denudation

This project builds upon previous denudation studies from each end and the middle of the San Juan River (Gillam, 1998; Wolkowinsky and Granger, 2004; Hoffman, 2009; McKeon, 2009; Karlstrom et al, 2012, Lee et al., 2012; Kelley and Karlstrom, 2017). To infer long-timescale denudation, thermochronology samples have been collected in the upper (McKeon, 2009; Kelley and Karlstrom, 2017), middle (Hoffman, 2009), and lower (Lee et al., 2012) reaches of the San Juan drainage (Figure 1). These thermochronology data provide a long record of the differential denudation of this area. Geologic evidence for long term denudation amounts is also shown in Figure 2 in terms of elevations of Laramide and Oligocene laccoliths that were emplaced as shallow intrusions in the Cretaceous section and that now form “sky islands” in the landscape, and by 35 and 27 Ma erosion surfaces below and above the Chuska Sandstone in the Chuska Mountains (Cather et al., 2008).

Thermochronology data from eastern Grand Canyon (see summary in Karlstrom et al., 2020) include modeled temperature- time (T-t) paths from five river-level samples from Marble Canyon that are summarized using weighted mean paths of Karlstrom et al. (2014, their Fig. 2A). Assuming a geothermal gradient of 25 °C/km and a surface temperature of 15 °C, Lee et al. (2012) used AFT and apatite (U-Th)/He thermochronology to conclude that 1.7 to 2.2 km of Mesozoic strata remained above the area of Lees Ferry until after 5 Ma. Figure 2 reconstructs the relative magnitudes of denudation of these river-level samples. Sample 1, at

Lees Ferry, was at ~ 60 °C at 5 Ma corresponding to a burial depth of 1.8 km; sample 2 was at ~ 50 °C corresponding to a depth of 1.4 km. In contrast, samples 3 and 4 had cooled to 20-30 °C by 15 Ma and were buried only 400-800 m at 5 Ma (Lee et al., 2012). Miocene cooling observed in some samples records carving of the 25-15 Ma East Kaibab paleocanyon below the Colorado – Little Colorado River confluence as shown in sample 4 (Karlstrom et al., 2017, their Fig. 3) and cooling at ~ 15 Ma in sample 3 was related to the northward retreat of the Vermillion cliffs past this sample. Using different mean annual surface temperature and geothermal gradient assumptions results in different temperature-to-depth conversions but the relative long-term differential denudation recorded by these samples is robust and suggests the presence of a paleo Vermillion cliffs such that the San Juan River system had not been integrated through Marble Canyon to the East Kaibab paleocanyon (paleo-Little Colorado River) before 5 Ma.

Thermochronology studies from the Monument uplift on the San Juan River by Hoffman (2009) reported apatite (U-Th)/He thermochronology from surface and core samples (Figure 2) that indicate rapid cooling since ca. ~ 6 Ma. Hoffman used a geothermal gradient of 30 °C/km and mean annual surface temperature of 10 °C to estimate 1.5-2.0 km of erosion since the late Miocene (4-10 Ma) at rates of 230-300 m/Ma.

At the headwaters of the San Juan River north of Durango, Colorado, McKeon (2009) analyzed samples using apatite (U-Th)/He thermochronology. Results showed a rapid cooling event that commenced ca. 10–6 Ma in the northwestern San Juan Mountains whereas in the southern San Juan Mountains there were significantly older cooling ages from 32–19 Ma (Figure 1). McKeon (2009) and Karlstrom et al. (2012) suggested that the variability in

exhumation between the northwestern San Juan Mountains and southern San Juan Mountains is due to active tectonism in the northwest region of the San Juan Mountains because the areas are similar in climatic history, mean elevation, and relief. These results suggest about 2 km of differential erosion via epeirogenic doming in the southwestern San Juan Mountains. Kelley and Karlstrom (2017) analyzed samples using apatite fission-track (AFT) thermochronology near Molas Pass, north of Durango, Colorado, that also show a rapid cooling pulse at 10–6 Ma with more than a kilometer of material removed from above the 3300 m elevation sample since ~ 6 Ma.

These thermochronology results from the eastern Grand Canyon to the San Juan River headwaters constrain the age of initial integration of the San Juan/Colorado river system through Marble Canyon to have been after 6-5 Ma and indicate that the San Juan/Colorado system likely flowed across Cretaceous rocks, 1-2 km higher in the stratigraphic section, perhaps towards internally drained lakes (Lazear et al., 2013, their Fig. 10). Thus, the birth of the San Juan River as we know it today is considered in this paper to have been after, and perhaps to have helped drive, the 6-5 Ma integration of the Colorado River through Grand Canyon. Figure 2 estimates the 5 Ma paleosurface such that any pre-5 Ma San Juan River that may have flowed across the Four Corners region would have been at or above the elevation of Cretaceous strata now exposed in the Straight Cliffs and Black Mesa.

METHODS

Single Crystal $^{40}\text{Ar}/^{39}\text{Ar}$ Dating of Detrital Sanidines in River Terraces

River terrace samples were collected from terrace flights in several reaches of the Colorado and San Juan rivers. Sanidine grains were concentrated by sieving for grains

ranging from 250 - 125 microns, washed using distilled water and hydrochloric or hydrofluoric acid, magnetically separated with a Frantz magnetic separator, and put through standard heavy-liquid mineral separation to float the K-feldspars. Approximately 200 -300 sanidine grains were handpicked under a polarizing binocular microscope from the bulk K-feldspar population from each sample while submerged in wintergreen oil. Sanidine grains were irradiated at either the Oregon State University Triga reactor or USGS Triga reactor, Denver, CO along with standard Fish Canyon Tuff sanidine (FC-2) with an assigned age of 28.201 Ma (Kuiper et al., 2008). The ^{40}K decay constant used for age calculation is $5.463\text{e-}10$ /a (Min et al., 2000). Individual sanidine grains underwent $^{40}\text{Ar}/^{39}\text{Ar}$ dating by single crystal laser fusion with a CO_2 laser while gases were measured on an ARGUS VI noble gas mass spectrometer. Samples were analyzed at the New Mexico Geochronology Research Laboratory located at the New Mexico Bureau of Geology and Mineral Resources in Socorro, New Mexico. A maximum depositional age (MDA) is derived by calculating the weighted inverse variance mean age of the youngest population of dates per sample as described in Heizler et al. (2021).

$^{40}\text{Ar}/^{39}\text{Ar}$ dating of detrital sanidine crystals allows for precise ages and can help determine the source of ancestral river deposits. The assigned date of a sanidine represents an eruption age. The age of the youngest population of detrital sanidine crystals that has been reworked into a river terrace provides a maximum bound on the depositional age (the terrace can be no older than its youngest sanidine). Precise ages alone are sometimes enough to pinpoint eruptive sources, but K/Ca ratios (proportional to $^{37}\text{Ar}/^{39}\text{Ar}$) can also help identify sources (Deino and Potts, 1990; Karlstrom et al., 2017; Heizler et al., 2021). If maximum depositional ages increase systematically in higher and older terraces in terrace flights, it is

possible that these maximum depositional ages may approximate true depositional ages; they thus provide some of the best constraints on hypotheses for incision rates through time (Aslan et al., 2019). The confidence in the maximum depositional ages derived from the youngest detrital sanidine grains increases when more grains of a given young population are found, but even when $n=1$ young grain, our experience indicates that additional analyses generally produce more grains of that age such that we report $n=1$ results with reasonable confidence that they provide useful constraints that can be further tested (see discussion in Heizler et al., 2021 and Schaen et al., 2020).

RESULTS

Terrace Characterization

This section describes a synthesis of new and published data for flights of terraces, working upstream from eastern Grand Canyon, through Marble Canyon, Glen Canyon, the San Juan- Colorado river confluence, middle reaches of the San Juan River, and the Animas headwater tributary to the San Juan River. Several dating methods were previously used to estimate the ages of terraces. Previously published ages are reported in this section whereas new detrital sanidine results are reported in the next section. Figure 3 summarizes terrace heights and published ages for ten reaches; for terraces reported with height ranges we plot the maximum terrace height. More complete data are compiled in DR Table 1.

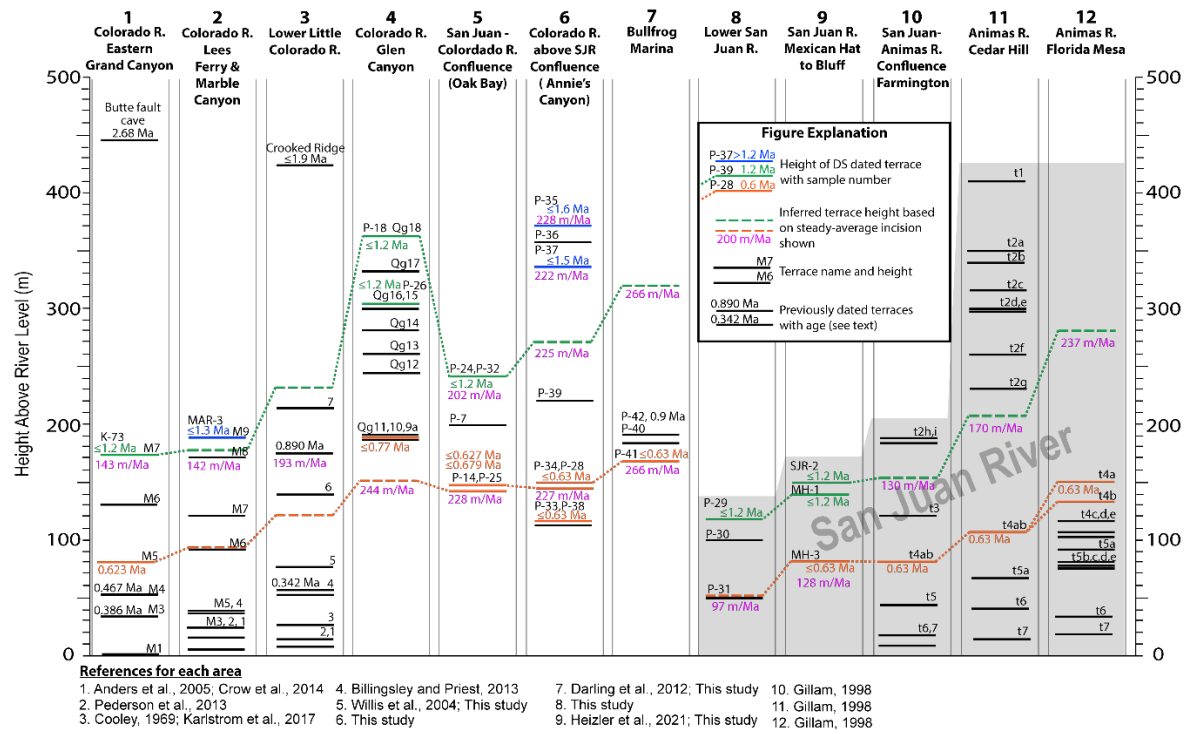


Figure 3 - Terrace correlation from previous workers compared to new, compiled, and dated terraces. Maximum heights of terrace ranges are shown. Bedrock strath heights above river level are plotted here for consistency with other reaches rather than bedrock strath heights above modern bedrock strath below river level as reported in Crow et al. (2014). Two major terraces, those containing 0.63 Ma Lava Creek B grains (orange) and terraces containing 1.2 Ma grains (green) are connected with orange and green dashed lines. This pair of terraces is about twice as high above the river in the Glen Canyon to San Juan confluence area (reaches 4 and 5) and in the Animas headwaters area (reaches 10 through 12) of the San Juan River relative to eastern Grand Canyon and Lees Ferry (reaches 1 and 2) and across the Colorado Plateau on both Colorado and San Juan rivers (reaches 5 through 9). Available age control suggests steady average incision rates in most reaches over the past 1.2 Ma but markedly different rates reach to reach. This indicates that terrace correlation at the regional scale cannot be based on terrace height above the river.

Eastern Grand Canyon: Eastern Grand Canyon incision rates were calculated previously from terrace flights at Kwagunt, Palisades, and Tanner side canyons, from river mile 57 to 69 (river miles are measured downstream from Lees Ferry). Terrace correlation and numbering (M1 to M7 refer to mainstem terraces) is from Anders et al. (2005). U-series

dates on travertine clasts and infillings combine to give direct ages on many terraces, and a strath-to-strath regression for M1 to M5 shows steady average incision rates of 160 m/Ma over the past 623 ka and perhaps for the past 2.68 Ma based on speleothem dating near RM 57 (Crow et al., 2014, their Figure 6). We test and build on the long term incision rate by new detrital sanidine dating of the highest preserved terraces (M9 at 172 m above river level) in eastern Grand Canyon near Unkar Rapids (RM 70), as described below.

Marble Canyon: Marble Canyon terraces of the Colorado River near Lees Ferry (Billingsley and Pierce, 2013) are plotted in Figure 3 using the terrace terminology of Pederson et al. (2013) and depicted in Figure 4. These workers reported optically stimulated luminescence (OSL) and terrestrial cosmogenic nuclide (TCN) results for terraces M1 to M5, with ages ranging from 23 ka to 142 ka and reported an incision rate of 350 m/Ma over the past 150 ka. Higher terraces were undated but extend to heights up to 189 m Above River Level (ARL) at Lees Ferry and 293 m ARL on the Kaibab rim of Marble Canyon. We applied detrital sanidine dating to the highest (M9) Johnson Mesa terrace (189 m ARL; shown by the yellow star in Figure 4) to test longer term average incision rates.

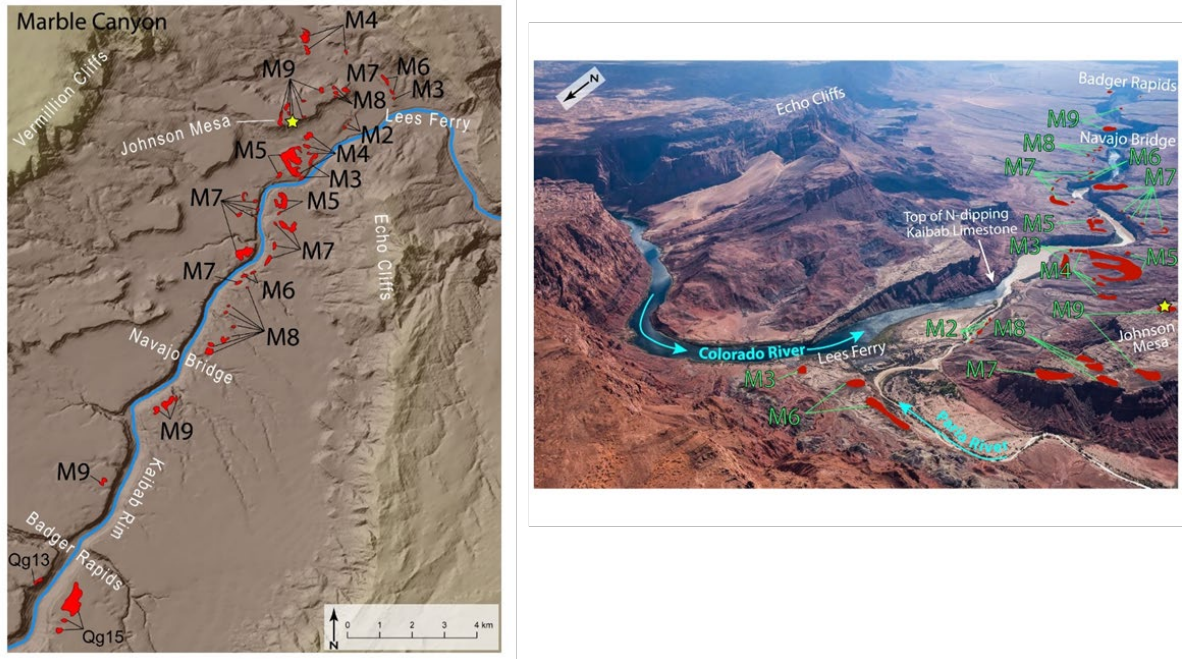


Figure 4 - Terrace maps and dated samples for upper Marble Canyon of Colorado River, RM 0 to ~ 8) generalized from Billingsley and Preist (2013) with lower Lees Ferry terraces from Pederson et al. (2013); also shown in a view looking south (photograph from Gary Ladd). Star on both maps is location of Johnson Mesa sample (MAR-3). Terrace heights are plotted above river profile in Figure 3, column #2.

Little Colorado River terrace heights were summarized by Cooley (1969, his Table 5) with age control summarized by Karlstrom et al. (2017). Most notably, these include the 57 m ARL strath and gravels beneath the 342 ka Tappan basalt flow and 172 m strath and gravels beneath the 890 ka Black Point basalt that yield incision rates of 167 and 193 m/Ma, respectively. Although less well constrained due to different projection interpretations, the height of the ≤ 1.9 Ma Crooked Ridge paleoriver above the Little Colorado River yields incision rates of 188-213 m/Ma relative to the confluence of the Little Colorado River and Moenkopi Wash (Karlstrom et al., 2017, their Figure 14) or 150 m/Ma relative to the profile of modern Moenkopi Wash (Heizler et al., 2021, their Figure 11). Collectively, these data suggest steady average incision rates that may be somewhat faster than rates in Eastern

Grand Canyon (Figure 3) and suggest an acceleration of incision in the past 2 Ma in the lower Little Colorado River, below its prominent knickzone (Karlstrom et al., 2017).

Glen Canyon: Glen Canyon terraces of the Colorado River in the area now flooded by lower Lake Powell are depicted in Figure 5 (in part from Billingsley and Pierce, 2013). These were undated prior to our detrital sanidine sampling which included the highest terraces at Page airport and Wahweap Marina (up to 323 m ARL), Cummings Mesa (280 m ARL), and Antelope Point (188 m ARL). The maximum filling of Lake Powell in 1980 is recorded by a bright white “bathtub ring” stain made by a thin carbonate coating that provides a horizontal datum at an elevation of 1126 m (Figure 6). The depth of the lake varies from ~132 m (as of 2021, ~41 m below maximum depth) at Glen Canyon Dam to zero where the lake meets the inflowing San Juan and Colorado rivers. Our datum for estimating incision rates is based on the Birdseye et al. (1922) survey of the pre-Dam river profiles for reporting the pre-Dam height of terraces ARL, with current heights measured relative to the 1126 m elevation of the top of the “bathtub ring”. Terraces below this “bathtub ring” have mostly been flooded by Lake Powell and those that have been re-exposed by low lake levels were generally not used for this study to eliminate the possibility of lake-reworked grains. Sampling was conducted in the spring of 2017, 2020, and 2021 that included Colorado River terrace sands with a range of terrace heights ARL from 112 m to 370 m (Figure 5).

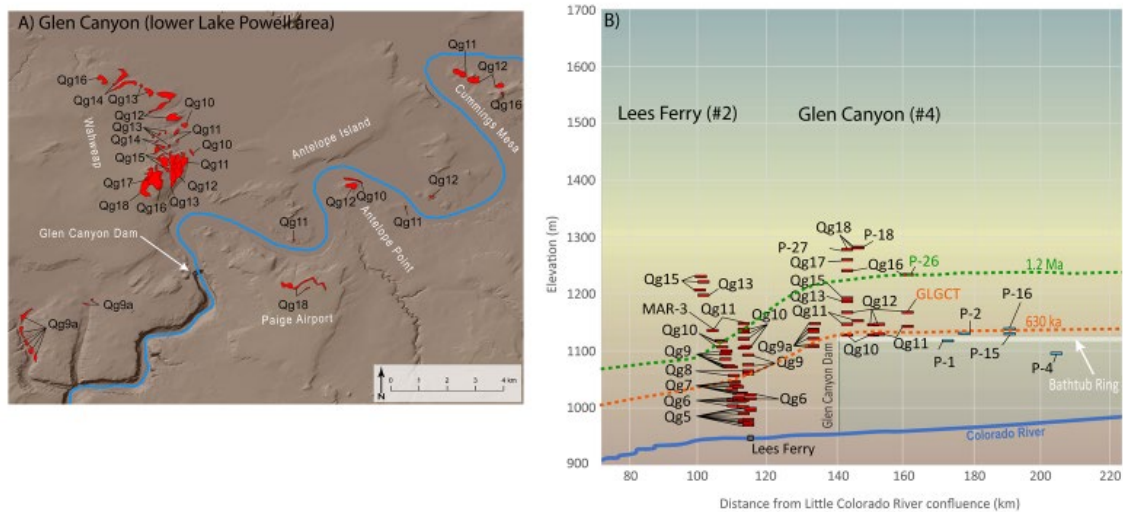


Figure 5 - A) Terrace maps and dated samples for Glen Canyon of the Colorado River, above Glen Canyon Dam and below the San Juan confluence. B) Profile view relative to both pre-Dam river elevation (blue line) and Lake Powell maximum water level (white line) for both the Lees Ferry area and Marble and Glen Canyon, columns #2 and #4, respectively, in Figure 3.

San Juan- Colorado River confluence: Terraces near the Colorado-San Juan river confluence (Figure 6) include the Cha surface pediment on the north side of Navajo Mountain that interfingers with river gravels at a height of 243 m ARL and lower terrace straths present at 199 and 143 m ARL. Garvin et al. (2005) reported ^{10}Be cosmogenic surface ages of 581 ± 130 ka for the Cha surface (at 4103-foot hill) and 266 ± 60 Ma at Oak Island, as well as 340 ± 54 and 222 ± 85 ka U-series ages on pedogenic carbonates from these gravels. This led to a hypothesis for very high incision rates of 400-700 m/Ma for these terraces. Karlstrom et al. (2013) considered these ages to be minima and hence incision rates to be maxima for the terrace straths as can be tested by the new detrital sanidine results presented below. Willis (2004) also mapped terraces at the Colorado-San Juan River confluence region and up the San Juan River as summarized in Table DR-1.

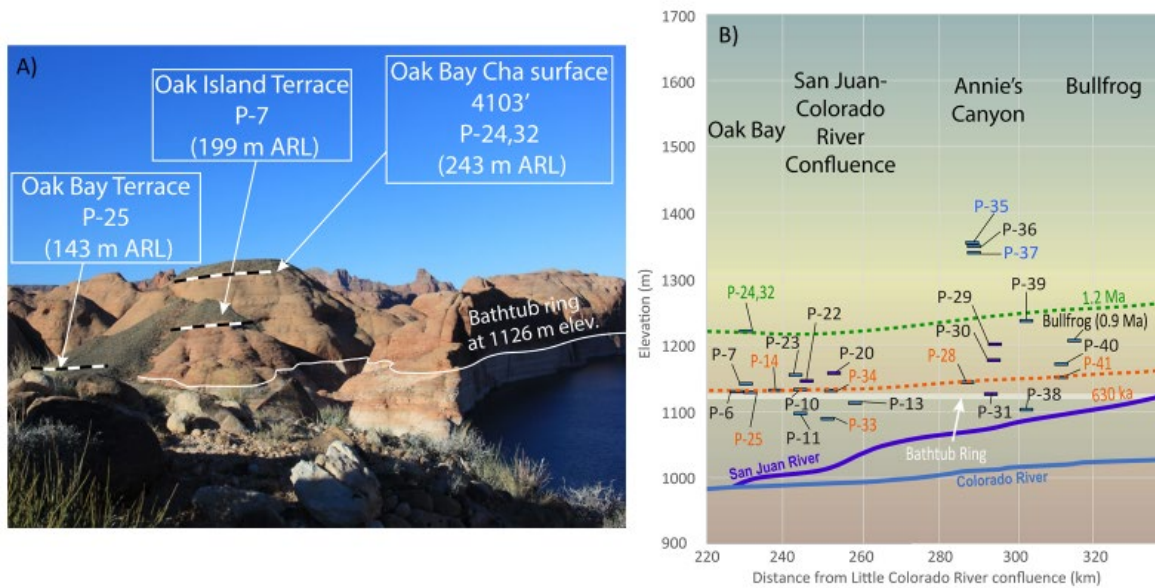


Figure 6 - A) Stacked high terraces in Oak Bay near the Colorado-San Juan river confluence include a location where the Cha surface pediment on the north side of Navajo Mountain interfingers with river gravels, an intermediate terrace on Oak Island, and a terrace just above the level of the bathtub ring in Oak Bay at 143 m ARL. B) Profile view of sampled terraces near the confluence, also shown in column #5 in Figure 3.

Colorado River above San Juan-Colorado River confluence: In upper Lake Powell terraces are present on the Colorado River near Annie’s Canyon (area 6 of Figure 3) and Bullfrog Marina (area 7). Previous dating has led to conflicting interpretations. Pederson et al. (2013, their Figure 4) used TCN rates of 420-450 m/Ma over the past few hundred thousand years from Glen Canyon to Canyonlands (Davis et al., 2001; Garvin et al., 2005; Marchetti and Cerling, 2005; Cook et al., 2009; Burnside, 2010) to propose a “central Colorado Plateau bull’s-eye of rapid incision” centered near the Henry Mountains. Darling et al. (2014) published an $^{26}\text{Al}/^{10}\text{Be}$ cosmogenic burial age of 1.5 Ma age for a 189 m side-

stream terrace giving an incision rate of 126 m/Ma. A reanalysis of the $^{26}\text{Al}/^{10}\text{Be}$ cosmogenic burial isochron was done that excluded an outlier of the isochron; this yielded a new age of 0.92 ± 0.30 Ma, with an MSWD of 0.13, giving a new incision rate of 205 ± 67 m/Ma (unpublished, Granger, D., 2021). Karlstrom et al. (2013) cited the 1.5 Ma cosmogenic burial age and suggested that the apparent bullseye reflected only short term incision rates. Additional DS dating of the Annie's Canyon and Bullfrog terraces can help test these alternatives.

San Juan River above Colorado River confluence: In upper Lake Powell, terraces are present at the Great Bend (area 8) and there are locally extensive terraces at Mexican Hat and Bluff (area 9). Wolkowinsky and Granger (2004) published an $^{26}\text{Al}/^{10}\text{Be}$ cosmogenic burial age of $1.36 + 0.20/-0.15$ Ma age for gravels that overlie the 151 m terrace strath near Bluff giving a bedrock incision rate of $110 +12/-16$ m/Ma. This was refined by Heizler et al. (2021) who reported an $^{40}\text{Ar}/^{39}\text{Ar}$ detrital sanidine age (a maximum depositional age for the terrace) of 1.199 ± 0.008 Ma for this same gravel yielding an incision rate of ≥ 125 m/Ma. Additional terrace samples were taken in these locations, plus at Mexican Hat, UT.

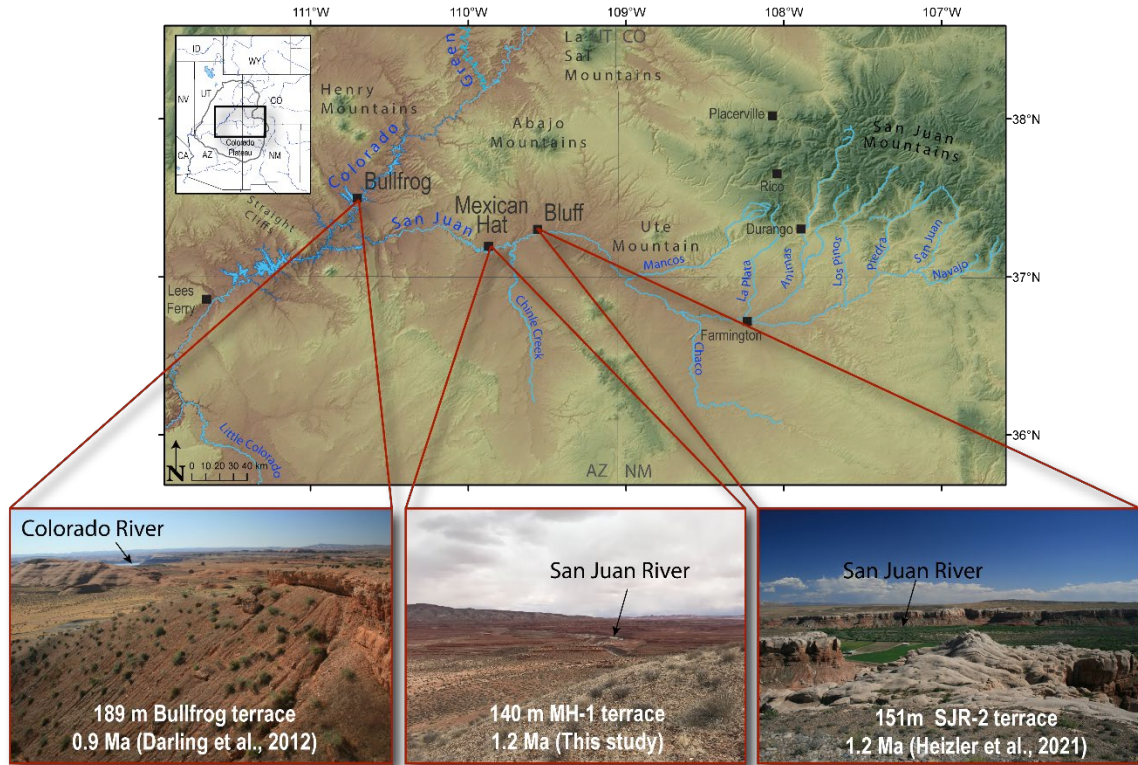


Figure 7 - Terraces at Bluff and Mexican Hat on the San Juan River and at Bullfrog Marina on the Colorado River test the incision rates of these rivers as they cross the central Colorado Plateau. Note that the 0.9 Ma age of the Bullfrog Marina terrace is modified here from the originally reported age of 1.5 Ma (Darling et al., 2012).

Animas River/ Upper San Juan River: In the headwaters of the San Juan River, Figure 8 shows terrace mapping along Animas River simplified from Gillam (1998). The lower reaches are near the confluence between the Animas and San Juan rivers near Farmington, NM, and the upper reaches extend up the Animas Valley north of Durango and into the Needle Mountains. Eight different groups (ages) of terraces were correlated within the Animas Valley along with four differentiated subgroups that were characterized by lateral continuity, height differences between horizontally eroded bases, and degree of soil development. Gillam (1998) reported that the 0.630 Ma Lava Creek B ash (date of Jicha et al., 2016) overlies and is present within the t4a and t4b terraces. These terraces diverge

significantly upstream indicating upstream rates of > 200 m/Ma relative to downstream rates of 130 m/Ma, as shown in Figure 8. Additional detrital sandine samples were collected to further test this hypothesis.

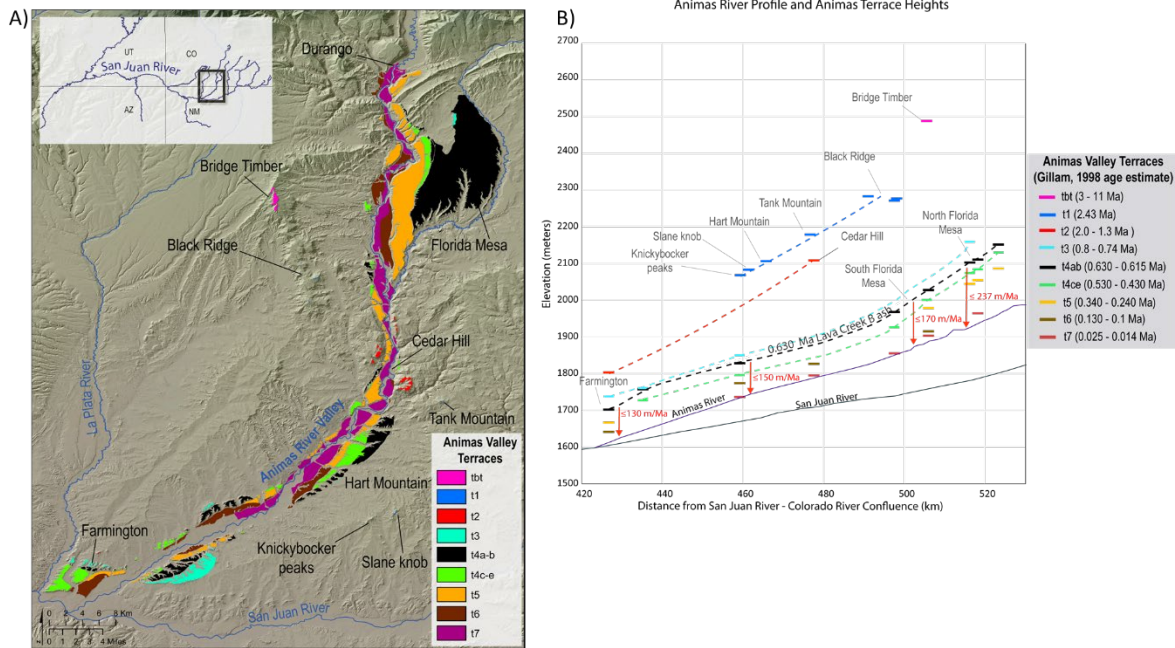


Figure 8 - A) The Animas Valley from the San Juan-Animas River confluence near Farmington, NM, to Durango, CO. Terraces mapped by Gillam (1998) were digitized in ArcGIS and labeled from youngest t7 to oldest tbt. Terrace t8 is north of Durango and not included in this map. B) River profile of the Animas River from Farmington, NM, to Durango, CO. Terrace t4ab is directly overlain by Lava Creek B ash (630 ka; cf. Jicha et al, 2016); its strath is estimated using 10 m USGS DEM elevations and maximum local gravel thicknesses at the north end of Florida Mesa, southern end of Florida Mesa, near Cedar Hill, NM and Farmington, NM. Other terrace group heights are estimated using a 10m USGS DEM and geographic location based on Gillam (1998). Terrace ages were estimated by Gillam (1998): t4ab terrace heights and estimated river incision imply that terraces diverge upstream and incision rates increase upstream from 130 m/Ma to 237 m/Ma.

Detrital Sanidine Results

Table 1 - RIVER TERRACES DATED WITH DETRITAL SANIDINE IN THIS STUDY

Sample #	Map name	River	Name Location	Latitude	Longitude	GPS Elevation (m)	Strath height above Birdseye et al (1920) paleo river and modern river (m)	Age of youngest grain(s) (Ma)	Error 1σ (Ma)	MSWD	# of youngest grain (n)	Total # of grains dated (N)	Minimum incision rate relative to river (m/Ma)
K17-73	K-73	LC	Unkar below Basalt Canyon	36.07111	-111.88168	934	172	1.212	0.026	NA	1	475	142
K16-MAR-3	MAR-3	LC	Johnson Mesa	36.86211	-111.61338	1139	189	1.329	0.009	2.75	2	153	142
K20-POW-27	P-27	LC	Wahweep Bay High: View Point	36.96684	-111.49990	1280	323	74.5	0.2	2.8	2	97	4
K17-POW-18	P-18	LC	Page Airport	36.93373	-111.44632	1282	325	1.203	0.036	5.66	5	57	270
GLG-CT	GLG-CT	LC	Antelope Point	36.965	-111.436	1146	188	0.768	0.044	NA	1	435	245
K20-POW-26	P-26	LC	Cummings Mesa	36.99244	-111.39019	1246	280	1.232	0.016	0.50	3	162	227
K20-POW-24	P-24	LC	S. 4103 Oak Bay #1	37.19690	-110.89388	1200	243	3.342	0.059	NA	1	354	73
K21-POW-32	P-32	LC	S. 4103 Oak Bay #2	37.118993	-110.96358	1224	243	1.237	0.034	0.88	3	239	197
K17-POW-7A	P-7	LC	Oak Island	37.12543	-110.95294	1142	199	10.41	0.20	NA	1	145	19
K20-POW-25	P-25	LC	Low Oak Bay	37.11611	-110.95922	1105	143	0.627	0.012	2.170	11	150	228
K17-POW-14	P-14	LC	Hidden Passage	37.16824	-110.93148	1132	149	0.679	0.006	1.140	47	220	219
K21-POW-33	P-33	UC	Hole in the Wall Low	37.24754	-110.8833	1090	112	0.682	0.012	1.64	8	196	164
K21-POW-34	P-34	UC	Hole in the Wall High	37.25084	-110.88098	1132	149	0.628	0.005	1.20	23	206	237
K21-POW-28	P-28	UC	Annie's Canyon Low	37.35656	-110.73051	1145	145	0.636	0.006	1.73	17	208	228
K21-POW-35	P-35	UC	Annie's Canyon High #1	37.36657	-110.74237	1355	370	1.618	0.010	1.92	9	218	229
K21-POW-37	P-37	UC	Annie's Canyon High #3	37.3712	-110.74116	1341	334	1.504	0.015	NA	1	275	222
K21-POW-39	P-39	UC	Near Lake Canyon High	37.43126	-110.7139	1238	221	8.033	0.064	NA	1	253	28
K21-POW-41	P-41	UC	Near Bullfrog Marina Low	37.47029	-110.72921	1152	168	0.634	0.028	2.13	3	42	265
K21-POW-42	P-42	UC	Bullfrog Marina	37.520	-110.700	1200	189	34.04	0.14	NA	1	126	6
K21-POW-29	P-29	SJ	SJR Big Bend High #1	37.26361	-110.69614	1202	118	1.221	0.019	NA	1	199	97
K21-POW-31	P-31	SJ	SJR Big Bend Low #3	37.26667	-110.70048	1127	51	7.42	0.06	NA	1	286	7
SJR21-MH-1	MH-1	SJ	Mexican Hat High	37.15945	-109.88114	1373	140	1.236	0.016	1.67	5	258	113
SJR21-MH-3	MH-3	SJ	Mexican Hat Low #2	37.15357	-109.8621	1322	82	0.640	0.034	NA	1	230	128
SJR-DZDS-2	SJR-2	SJ	Bluff Gravel Quarry	37.2982	-109.54904	1453	151	1.208	0.008	1.580	14	256	125
MA20-ANI-4	A-4	A	Slane Knob; Gillam (1998) t1u	36.82319	-107.86655	2065	334	8.45	0.10	NA	1	144	40
MA20-ANI-6	A-6	A	Arch Rock Canyon; Gillam (1998) t4b	36.89795	-107.88161	1865	97	16.128	0.056	NA	1	136	6
MA20-ANI-5	A-5	A	Cedar Hill area; Gillam (1998) t2f	36.9827	-107.89297	2057	260	9.50	0.12	NA	1	95	27

LC = Lower Colorado River below Colorado-San Juan River confluence; UC = Upper Colorado River above Colorado-San Juan River confluence; SJ = San Juan River; A = Animas River

We present new detrital sanidine results for twenty-seven samples extending from the eastern Grand Canyon, up the Colorado and San Juan Rivers, to the Animas headwaters (Table 1). We dated over 5000 individual sanidine grains and obtained post- 2 Ma grains that provide new maximum depositional ages for 18 of the terraces. A comparisons of detrital sanidine spectra collected from the twenty-seven samples show sanidines dominated by ages of 40 – 20 Ma derived from the San Juan volcanic field (Figure 9). Young grains (< 2 Ma) that can constrain the maximum depositional ages were found in eighteen of the twenty-seven terraces (Table 1). The most common ages of the youngest grains were ~1.2 and ~0.6 Ma (Figure 10a and b). Figure 3 shows the terraces that contain either the ~1.2 Ma grains (in green) or the ~0.6 Ma grains (in orange). Also, Figure 3 interpolates where the ~0.6 and ~1.2 Ma terraces may be between other dated terraces. A first-order conclusion from this paper is

that each reach shown in Figure 3 has a different terrace “barcode” and that terraces with the same youngest grains, that are likely temporally correlatives, are at very different heights above the river.

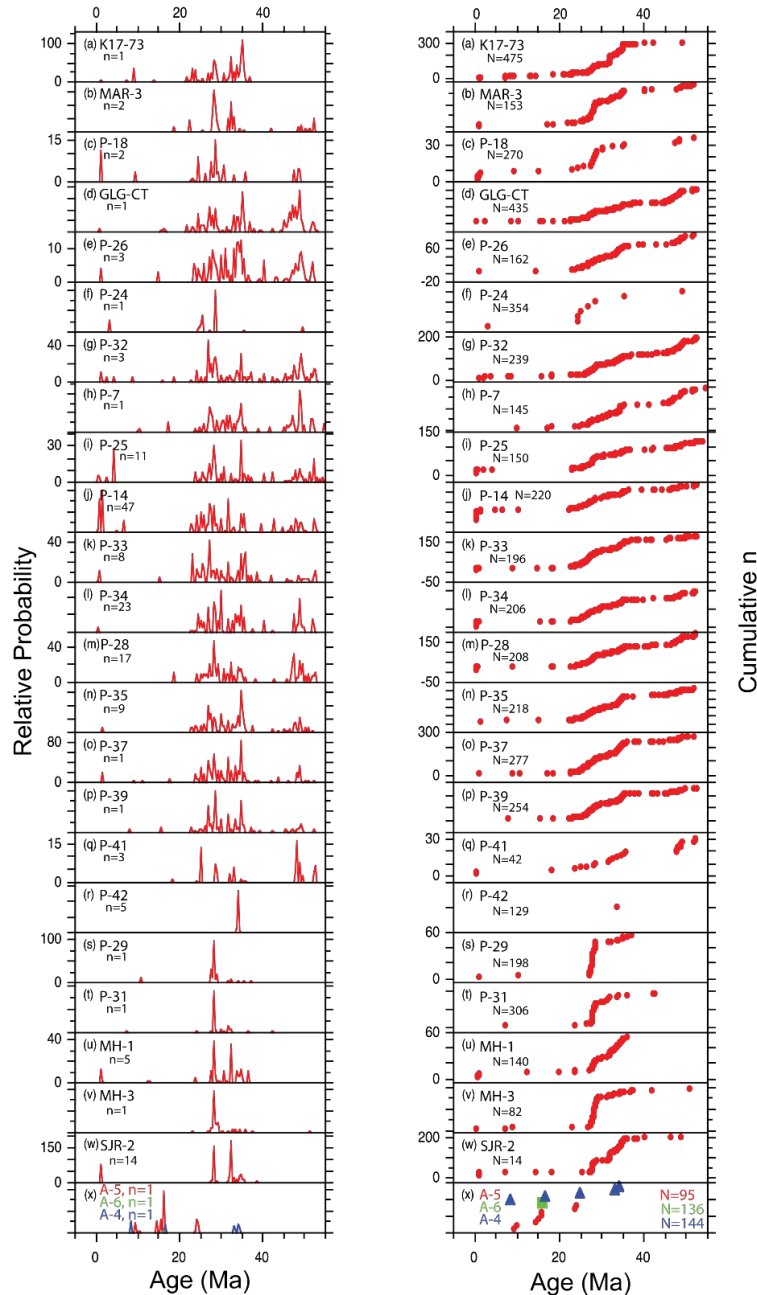


Figure 9 - Summary of 0-50 Ma detrital sanidine (DS) grains from the study area. The relative probability (left column) and cumulative number of DS grains (right column) for each sample is listed from downstream terraces (a) to upstream terraces (x). Animas samples in both columns (row x) are grouped together because they had very few DS grains and none younger than 6 Ma. Sample P-27 is not listed because there were no grains younger than 70 Ma. Note the prominent modes in all samples between 20 – 40 Ma. ‘n’ depicts number of grains defining the youngest population of dates whereas ‘N’ denotes total number of grains between 20 and 40 Ma.

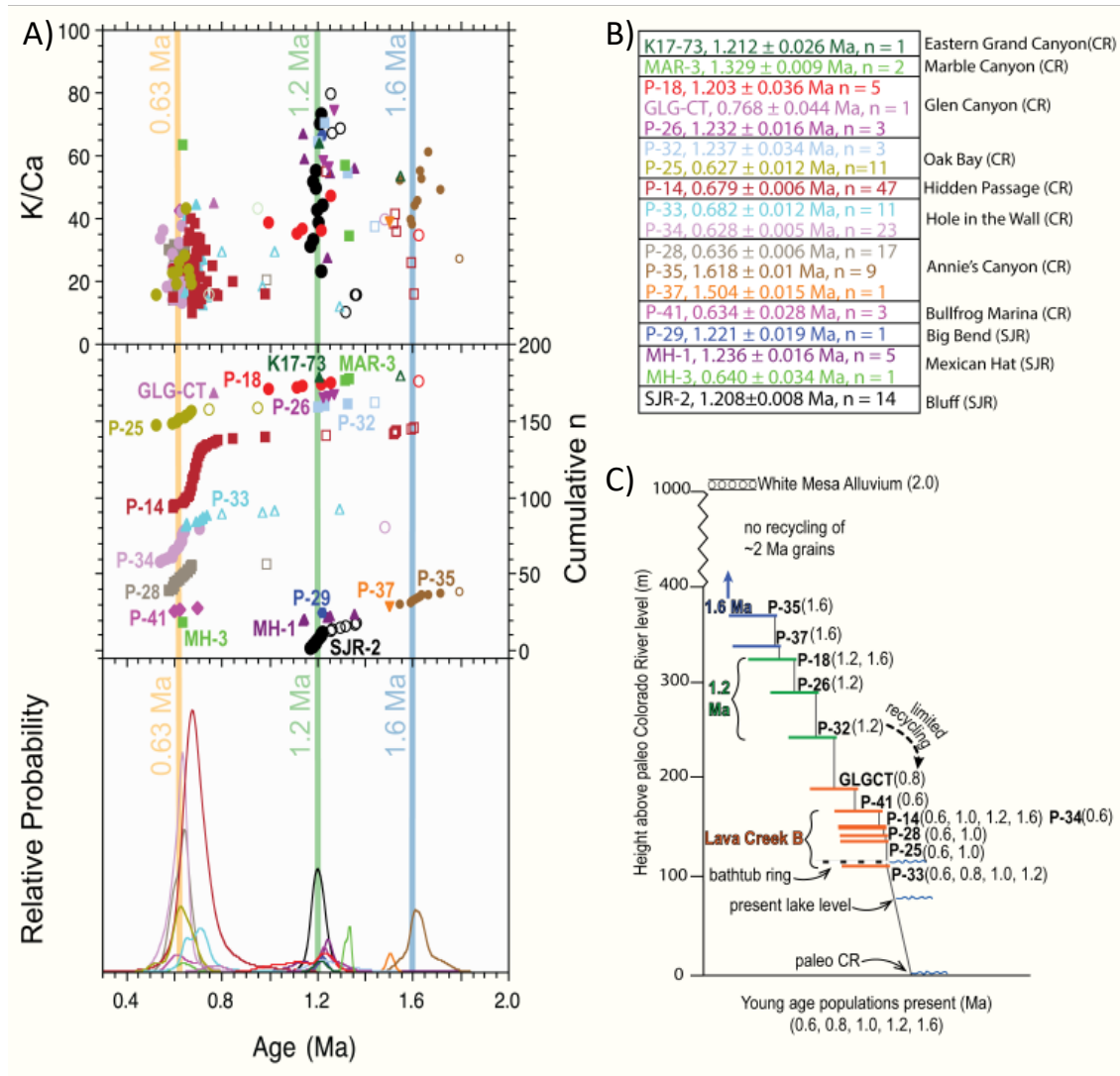


Figure 10 – A) Relative probability plots of $^{40}\text{Ar}/^{39}\text{Ar}$ analyses for youngest grain populations. The x-axes show age from 0.3 – 2.0 Ma and the distribution of sanidine ages per sample. Relative probability, number of grains analyzed, and K/Ca ratios are stacked on the Y-axes. Note the prominent modes at ~0.6 – 0.77 and ~1.2-1.3, and ~1.5-1.6 Ma that are used to correlate terraces from eastern Grand Canyon to the San Juan Mountains along the Colorado and San Juan Rivers. Unfilled symbols show grains that were omitted from the DS maximum depositional age calculation. B) Summary of 18 terraces with new DS maximum depositional ages. C) Schematic sketch of dated terraces in Glen Canyon (fast incision reach) showing heights of terraces and limited extent of grain recycling of young grains into lower terraces; main populations of young grains are (2.0, 1.6, 1.2, 1.0, 0.8, and 0.6 Ma)

Eastern Grand Canyon: A sample from the 172 m ARL terrace near Unkar Rapids

(RM 70) in eastern Grand Canyon yielded a youngest detrital sanidine grain of 1.212 ± 0.026

Ma (n= 1) that gives an incision rate of ≥ 142 m/Ma measured from river level, or ≥ 163 m/Ma measured from the ~ 25 m depth to bedrock beneath the Colorado River as calculated from strath-to-strath regression of nearby terraces (Crow et al., 2014). This supports models where eastern Grand Canyon has been incising at a steady average incision of ~ 160 m/Ma for the past 1.2 Ma, and perhaps for the past 2.68 Ma (Polyak et al., 2008; Crow et al., 2014).

Marble Canyon: MAR-3, the M9 terrace of Pederson et al. (2013), has a strath 189 m ARL near Lees Ferry on Johnson Mesa; it yielded youngest detrital sanidine grains of 1.329 ± 0.009 Ma (n=2) that give an incision rate of ≥ 142 m/Ma measured from river level and 155 m/Ma using the 17-m depth to bedrock known at Glen Canyon Dam (Karlstrom et al., 2007). M7 (Pederson et al., 2013), 80 m ARL near Cathedral Wash, and lower Johnson Mesa and Qg15 (Billingsley and Priest, 2013), 293 m ARL near Badger rapids are priority targets to further test for steady incision in the Lees Ferry reach of upper Marble Canyon. These sites were visited, but their thin gravel deposits could not be sampled.

Glen Canyon: There are four new detrital sanidine results for the Colorado River through Glen Canyon, below the Colorado-San Juan river confluence area and above Lees Ferry. About 750 individual sanidine grains were analyzed from these terraces. These four terrace samples are P-18, GLG-CT, P-26, and P-27. The youngest population of grains dated in P-18 (Page Airport) gave an MDA of 1.203 ± 0.036 Ma (n=5) for an incision rate of ≥ 270 m/Ma. GLG-CT (Antelope Point) yielded a grain at 0.768 ± 0.044 Ma (n=1) for an incision rate of ≥ 245 m/Ma. The youngest population of grains dated in P-26 (Cummings Mesa) gave an MDA of 1.232 ± 0.016 Ma (n=3) for an incision rate of ≥ 227 m/Ma. P-27 did not yield any grains younger than 70 Ma.

San Juan- Colorado River confluence: There are seven new detrital sanidine results for the San Juan-Colorado River confluence area. The seven samples analyzed were P-7, P-14, P-24, P-32, P-25, P-29, and P-31. P-7 produced no grains younger than 10 Ma. The youngest population of grains dated in P-14 (Hidden Passage) gave an MDA of 0.679 ± 0.006 Ma ($n=47$) for an incision rate of ≥ 219 m/Ma. The youngest grain dated in P-24 (S. 4103 Oak Bay #1) is 3.5 Ma ($n=1$) but the sample was mostly dominated by grains older than 10 Ma. The youngest population of grains dated in P-25 (lowest in Oak Bay) give an MDA of 0.627 ± 0.012 Ma ($n=11$) for an incision rate of ≥ 228 m/Ma. P-32 is a resampling of P-24, the highest terrace in Oak Bay at 243 m ARL. The MDA for P-32 is 1.237 ± 0.034 Ma ($n=3$).

Above San Juan-Colorado River confluence to Bullfrog: There are eleven terrace samples from above the San Juan-Colorado river confluence to Bullfrog Marina at Lake Powell. The samples are P-28, P-33, P-34, P-35, P-36, P-37, P-38, P-39, P-40, P-41, and P-42. Near Annie's Canyon P-28, P-35, P-36, and P-37 range from 145 m to 370 m ARL. P-28, a 145 m terrace, yielded an MDA of 0.636 ± 0.006 Ma ($n=17$) with an incision rate of ≥ 227 m/Ma. The MDA for P-35, a 370 m terrace was 1.618 ± 0.010 Ma ($n=9$) for an incision rate of ≥ 228 m/Ma. P-37, a 334 m terrace, yielded an MDA of 1.504 ± 0.015 Ma ($n=1$) for an incision rate of ≥ 222 m/Ma. P-33 and P-34 are near Hole in the Wall at Lake Powell at 112 m and 149 m ARL, respectively. P-33 yielded an MDA of 0.682 ± 0.012 Ma ($n=8$) for an incision rate of ≥ 164 m/Ma. P-34, the higher terrace at Hole in the Wall, yielded an MDA of 0.628 ± 0.005 Ma ($n=23$) for an incision rate of ≥ 237 m/Ma. P-38 and P-39 are near Lake Canyon at Lake Powell at 116 m and 221 m ARL, respectively. P-38 was not analyzed for this study and P-39 did not yield any grains younger than 8 Ma. P-40 and P-41 are near Bullfrog Marina at 183m and 163 m ARL, respectively. P-40 was not analyzed for this study.

P-41, the 168 m terrace, yielded an MDA of 0.63 ± 0.03 Ma ($n=3$), for an incision rate of ≥ 266 m/Ma. P-42 is from the Darling et al. (2012) site near Bullfrog airport at 189 m ARL. P-42 had scarce sanidine and only yielded a youngest grain at 34.04 Ma.

Mexican Hat to Farmington: The previously dated 151 m terrace, SJR-2, in Bluff, UT yielded cosmogenic burial isochron age of $1.36 +0.20/-0.15$ Ma (Wolkoinisky and Granger, 2014) and was also re-dated by Heizler et al. (2021) using detrital sanidine that yielded a MDA of 1.208 ± 0.008 Ma ($n=15$). This DS-derived MDA gives a minimum incision rate of ≥ 125 m/Ma that more precisely confirms the relatively slow rates proposed by Wolkoinisky and Granger (2004). These rates are also in agreement with rates of ~ 130 m/Ma in the past 0.63 Ma determined at Farmington, NM (Gillam, 1998) and support models for semi-steady incision in this reach over the past 1.2 Ma. At Mexican Hat, MH-1 and MH-3, with terrace heights ranging from 70 m to 140 m, were collected to further test for steady incision across the Monument uplift between Bullfrog and Mexican Hat. MH-1, a 140 m terrace, yielded an MDA of 1.236 ± 0.016 Ma ($n=5$), for an incision rate of ≥ 113 m/Ma. MH-3, an 82 m terrace, yielded an MDA of 0.640 ± 0.034 Ma ($n=1$), for an incision rate of 128 m/Ma.

Animas River/ Upper San Juan River: The Animas terrace samples we dated are ANI-4, ANI-5, and ANI-6 (Figure 3) with ~ 370 grains analyzed, collectively. In general K-feldspar grains were only somewhat clear with subtle microtextures when viewed while picking and, as supported by the abundance of Precambrian grains, most of the crystals were orthoclase rather than sanidine. In the Animas River valley samples, the vast majority of grains are older than 600 Ma and none yielded detrital sanidine ages less than 2 Ma. Sample

ANI-4, a 334 m terrace had a youngest grain at ca. 8.5 Ma while ANI-5 had a youngest grain at ca. 9.5 Ma. Sample ANI-6 underlies the 0.630 Ma Lava Creek B ash and despite the lack of young DS grains, this age represents its likely depositional age.

INTERPRETATION AND DISCUSSION

Interpretation of maximum depositional ages

Detrital sanidine dating of river terraces provides evidence for the degree of grain recycling from higher to lower terraces at locations along the Colorado and San Juan River systems. To evaluate recycling effects on DS MDAs, the terrace locations, their positions ARL, and the youngest grain ages for each terrace are shown in Figure 10a, b and c. There are two locations along the Colorado and San Juan River systems within the study area that show older grains recycled into lower terraces. 1) At the terminus of Glen Canyon, near Glen Canyon Dam, samples P-18 (325 m) and P-26 (280 m) that both contain young grains of about 1.2 Ma yet if you apply the steady incision rate of ~250 m/Ma, the higher terrace could be ~ 180 ka older. When the MDA for the higher terrace is either younger or has the same MDA as the next lower terrace, the higher terrace must be closer to the age of the young grain. Therefore, near Glen Canyon Dam, the 325 m terrace (P-18) represents the maximum depositional age at 1.2 Ma. 2) In Glen Canyon near Hole in the Wall, samples P-34 (149 m) and P-33 (112 m) both contain grains of about 0.63 Ma and using similar reasoning and a rate of 220 m/Ma the higher terrace could be ~ 170 ka older and the 149 m terrace (P-34) more closely approximates the 0.63 Ma Lava Creek B terrace.

However, the degree of recycling across the region is limited (Figure 10). The only terraces that contain both 1.2 and 0.6 Ma grains are P-14 and P-33. In most other areas, six of the ~0.6 Ma terraces do not contain 1.2 Ma grains and only three of the 1.2 or 0.6 Ma terraces contain grains from 2.3 to 2.7 Ma, and none contain the 2.0 Ma grains that are so abundant in the White Mesa Alluvium (Heizler et al., 2021). Our interpretation of this observation is that distribution of ash is greatest at or shortly following the time of a given eruption and the ash does not widely persist in the landscape or river system to be readily recycled into younger terraces. Thus, especially for terraces with numerous grains of the same age such as P-25, P-14, P-34, P-28, and SJR-2 the maximum depositional ages are likely to be close to the true depositional ages of the terraces.

Comparison of different age dating methods for river terraces

The likelihood that MDAs approximate true depositional ages (perhaps within 100-200 ka) is also supported in terrace flights where multiple dating methods have been applied. In eastern Grand Canyon, direct dating of terrace flights was done using U-series dating of both travertine clasts and infillings in gravels. A strath-to-strath regression of the age-height relationships from river miles 57 to 69 shows steady incision at 160 m/Ma relative to the modern bedrock under the river that also may apply over the past 2.68 Ma (Polyak et al., 2008; Crow et al., 2014). Our new MDA of 1.212 ± 0.026 Ma ($n=1$) from the 172 m ARL terrace near Unkar Rapids (RM 70) in eastern Grand Canyon gives a similar incision rate of ≥ 163 m/Ma compatible with the MDA approximating the true depositional age.

$^{26}\text{Al}/^{10}\text{Be}$ cosmogenic burial ages of river deposits represent direct dates on the time of deposition because the estimated age represents the time since the sediment was buried

(Granger, 2006). When this method is combined with detrital sanidine ages for the same terrace, the DS MDA is often within 2-sigma error of the direct cosmogenic burial age. For example, at Bullfrog Marina along the Colorado River and at Bluff, Utah along the San Juan River there are two locations that cosmogenic burial ages and DS MDAs can be compared. The Bullfrog Marina 189 m terrace gives a direct cosmogenic burial isochron age of 0.92 Ma \pm 0.60 Ma (2-sigma). The 21-m-lower 168 m terrace gives a DS MDA of 0.63 \pm 0.06 Ma (2-sigma). Thus, at 2-sigma uncertainty the age range of the 189 m terrace is 1.52 – 0.32 Ma. However, 168 m terrace's MDA gives an incision rate of \geq 266 m/Ma. Applying this rate to the 189 m terrace predicts a depositional age of \sim 0.7 Ma on the 189 m terrace, which is within error of the 0.92 Ma cosmogenic burial age and overall supports that the DS MDA is an approximation of the depositional age of the 168 m terrace.

At Bluff, Utah, Wolkowinsky and Granger (2014) dated the 150 m terrace and determined a $^{26}\text{Al}/^{10}\text{Be}$ cosmogenic burial age of 1.36 +0.20/-0.15 Ma (2 sigma). This is within error of the new 1.208 +/- 0.016 Ma (2 sigma) $^{40}\text{Ar}/^{39}\text{Ar}$ detrital sanidine MDA for the same gravel. The age range for deposition of this terrace that is compatible with both methods at 2- sigma would be 1.224 to 1.21 Ma. This comparison also indicates that the DS data provide a close estimate of the depositional age for this terrace.

Terrace correlation using detrital sanidine provenance and age

Detrital sanidine results show that terraces along the San Juan and Colorado rivers contain several major age populations of young grains, with modes of approximately ~0.63 Ma, ~1.2 Ma, and 1.6 Ma (Figure 10). Seven terraces in the various study areas have 0.63-0.77 Ma sanidine grains and two additional terraces in the Animas River Valley contain the ca. 630 ka Lava Creek B tephra (Figure 3). Five of the terraces have ~1.2-1.3 Ma sanidine, cosmogenic burial ages are ~1.36 Ma (Wolkowinsky and Granger, 2004) and ~0.9 Ma (Darling et al., 2012; unpublished, Granger, D, 2021), and two terraces have 1.6 Ma grains.

Pleistocene felsic caldera eruptions in western North America that covered the study area with ash are shown in Figure 11a. These eruptions include the 630 ka Lava Creek B, 1.30 Ma Mesa Falls, and 2.1 Ma Huckleberry Ridge ashes from Yellowstone, 0.77 Ma Bishop Tuff from Long Valley caldera in California, and 1.23 and 1.61 Ma upper and lower Bandelier Tuffs in New Mexico. Additional potential sanidine sources include the San Francisco Peaks and Mount Baldy volcanic fields of Arizona, but neither of these has been well characterized. The grain size of most of the DS grains is 250 - 150 microns thus raising the possibility that sanidine grains in the terraces are directly from ash fall tephra that was deposited contemporaneous with terrace formation or from direct drainage connection to volcanic source rocks. In Figure 11b, upper Bandelier DS grains from two separate samples show a normal distribution of grains at 1.233 Ma with some older grains that are either xenocrystic or contain variable amounts of excess argon hosted in melt inclusions, implying that a single tuff can be the source for more than one age of sanidine. This may also be recorded in the DS spectra such as sample SJR-2 where there is a skewed population of ca.

1.2 Ma ages with variable K/Ca values. Interestingly, P-14 has a strong population (n=47) of DS grains with a weighted mean age of 0.679 ± 0.006 Ma that does not match the age of Lava Creek B but does have K/Ca values that are consistent with Lava Creek B tephra. This is likely not a systematic analytical error in the DS data and thus could represent a large population of ~ 0.68 Ma crystals from a more local source such as the San Francisco Peaks volcanic field near Flagstaff, AZ. We note that P-33 also has a mode at 0.68 Ma based on n=11 crystals. Sample GLG-CT produced a single sanidine grain with a date of 0.768 Ma and K/Ca value of near 60, which are a good match with the Bishop Tuff. Sample MAR-3 produced a DS MDA of 1.329 Ma, which is significantly older than the 1.23 Ma upper Bandelier Tuff and could represent the Mesa Falls Tuff from Yellowstone. Interestingly, the large eruption associated with the Huckleberry Ridge Tuff (2.1 Ma), is not represented in this dataset nor in other regional studies (i.e., Heizler et al., 2021). The eruptive source for the large population of ~ 2.0 Ma grains identified in the White Mesa Alluvium (Heizler et al., 2021) is presently unknown.

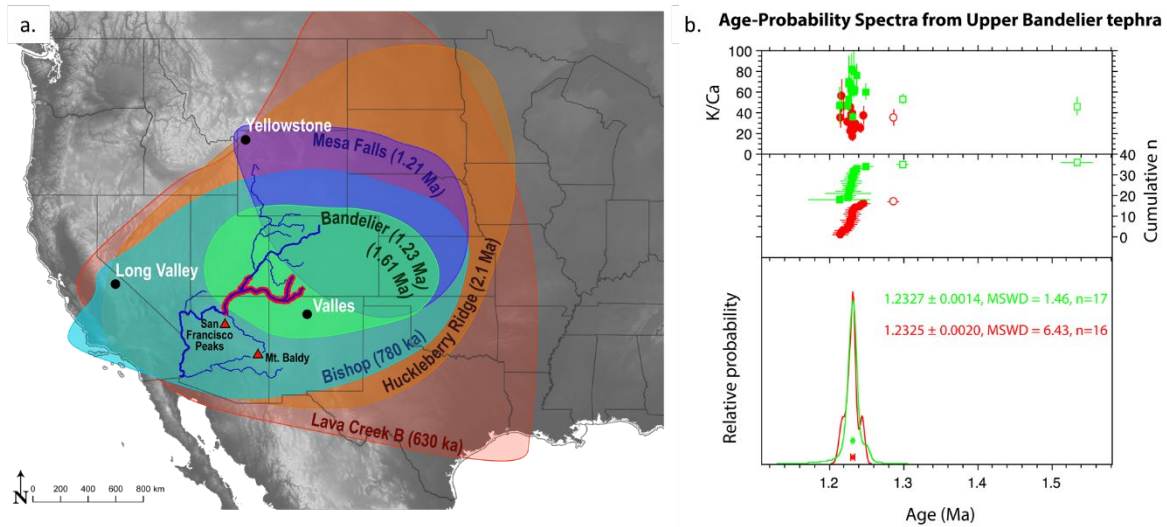


Figure 11 – A) Pleistocene felsic caldera eruptions in western North America that include sources from Yellowstone, Valles, and Long Valley calderas (black dots). The extent of contributing Yellowstone caldera eruptions includes Huckleberry Ridge, Mesa Falls, and Lava Creek B (Izett and Wilcox, 1982). The extent of Long Valley caldera eruptions includes the Bishop Tuff (Hildreth, 1979). The extent of contributing eruptions from the Valles Caldera includes the upper and lower Bandelier Tuff (Goff, 2010). Locations of the San Francisco Peaks and Mt. Baldy (red triangles) are among other potential sources of eruptions. Colorado River and major tributaries are shown by blue lines; the study area is highlighted in red. B) Relative probability spectra and $^{40}\text{Ar}/^{39}\text{Ar}$ DS analyses of youngest grain populations for the 1.23 Ma Bandelier Tuff (Zimmer, 2021, unpublished). Age in millions of years on the x-axes, relative probability, number of grains analyzed, and K/Ca ratios stacked on the Y-axes. Plots show sanidine ages with significant scatter, from 1.1 to 1.58 Ma, for two separate upper Bandelier Tuff samples.

Climatic influences on terrace development

Shifts between glacial and interglacial conditions and corresponding changes in water volume and sediment discharge are generally believed to influence fluvial terrace formation (Macklin et al., 2002; Bridgland and Westaway, 2008). Well documented glaciation in the headwaters of the Colorado and Animas-San Juan rivers (Guido et al., 2007; Johnson et al., 2017) makes it likely that climatic influences have affected terrace development at least to some degree in the study area. However, the compilation of mapped terraces and our proposed correlations based on the new DS MDAs suggest that connections between climatic

cycles and terrace formation and preservation in the study areas are complicated. For example, Figure 3 shows that at sites ranging from eastern Grand Canyon to the Animas River valley the number of terrace levels that are younger than ~ 0.6 Ma range from ~ 4 to 11 and that the number of levels that are younger than ~ 1.2 Ma range from ~ 6 to 16. This wide range of mapped terrace levels and the lack of any consistency or systematic change in the number of terrace levels upstream or downstream along the Colorado-San Juan River system strongly suggests that the different terrace levels have not formed simply in response to glacial-interglacial climate cycles.

Westaway et al. (2009) as well as other workers suggest that climatic effects on fluvial terrace development are best observed by comparing ages of terraces and Late Cenozoic climate events. For example, studies suggest that the ca. 3 Ma Mid-Pliocene climatic optimum (MPCO) (Van den Berg and Van Hoof, 2001; Westaway, 2001, 2002) and the ca. 1 Ma Middle Pleistocene Transition (MPT) (Van den Berg and Van Hoof, 2001; Antoine et al., 2007; Bridgland and Westaway, 2008) accelerated Late Cenozoic fluvial incision and produced distinct down-stepping flights of fluvial terraces within well-defined valleys globally. Figure 3 shows that most of the fluvial terraces in the study areas are younger than 1.2 Ma. This observation could reflect effects of the MPT event - specifically the transition to eccentricity-driven, large-amplitude ~ 100 ka glacial cycles. Similarly, Figure 3 could be interpreted to suggest that all the fluvial terraces in the study areas are younger than ~ 1.9 Ma. Long-term landscape denudation (lack of preservation) could explain the absence of terraces older than ca. 2 Ma. Alternatively, pre-2 Ma terraces may not have formed and terraces younger than ~ 2 Ma may reflect the advent of glacial-interglacial cycles and their influence on river hydrology and sediment discharge. Additionally, the noteworthy

presence of terraces with DS MDAs of ca. 0.6 and 1.2 Ma across the study areas suggests that there may be a connection between large-scale volcanic eruptions, landscape instability, and fluvial terrace formation. For instance, the Yellowstone eruption that produced the 0.63 Ma Lava Creek B tephra occurred during MIS 16, which was a prominent glacial cycle (Sarna-Wojckicki et al., 1987; Dethier, 2001). It is conceivable that the effects of the eruption contributed to removal of vegetation and destabilization of the landscape, and thus contributed to or amplified climatic influences on terrace development at this time. This would help explain why there are a significant number of alluvial deposits in the western U.S. that contain the Lava Creek B tephra (Izett and Wilcox, 1982).

In summary, we suggest that the new DS MDAs lend some support to the idea that the <2 Ma fluvial terraces in this region may record the effects of glacial-interglacial cycles. However, additional age constraints are needed to better resolve the effects of climate on fluvial terrace formation in comparison to other factors such as uplift.

Paleoprofile Synthesis

Our new incision rate synthesis within the Lees Ferry knickzone region, from eastern Grand Canyon to above Lake Powell along both the Colorado and San Juan River, is shown in Figure 12. Given the relatively common ~ 1.2 and ~ 0.6 Ma detrital sanidine ages we have found in these terraces, Figure 12 reconstructs paleo-profiles for these two timeframes, shown in green (1.2 Ma) and orange (0.6 Ma) relative to the modern river profile. In all reaches where dates of both ages have been obtained, the MDAs are consistent with the inset position of terraces, and the ~0.6 Ma paleoprofile is about half the height of the ~1.2 Ma paleoprofile, lending support to previous incision studies that also show steady average

bedrock incision rates in eastern Grand Canyon (Crow et al., 2014), the upper Colorado and San Juan rivers (Darling et al., 2012; Heizler et al., 2021), and the Little Colorado River (Karlstrom et al., 2017). This working hypothesis can be further tested with additional dating of the numerous terraces shown in Figures 5, 6 and 7 and especially those shown by gray bars in Figure 12 that either yielded no young grains or were especially difficult to sample so that we were unable to get undisturbed sand from the terrace deposit. It also suggests a need for additional incision data between Lake Powell and Canyonlands.

Between dated terraces, green and orange dots are the interpolated heights of the position of the 0.6 and 1.2 Ma terraces using the incision rates shown and assuming the MDAs approximate depositional ages. These paleoprofiles show that in the six areas where there are data from multiple terrace heights (Fig. 12), incision rates have remained steady in each of the reaches over the past ~1.2 to ~1.6 Ma. Rates at and below the Lees Ferry Kaibab limestone knickpoint average 148 m/Ma relative to the river (160 m/Ma relative to bedrock); rates on the Colorado River above the knickpoint are faster and range from 202-270 m/Ma with an average of 237 m/Ma; and rates on the San Juan River 60-250 km above the confluence show the slowest incision rates of 97 to 128 m/Ma with an average of 113 m/Ma.

These results are not compatible with the model of Cook et al. (2009) who predicted non-steady rates as a transient incision wave passed a given point, at least not in the past ~500 ka as they used to illustrate the model. The data also do not support Pederson et al.'s (2013, their Fig. 4) "bullseye of incision" in that our observed long-term rates are about half their proposed 350-420 m/Ma rates measured over several hundred ka above the knickzone and do not show a northward increase in incision rates. The data also do not support the

model of Karlstrom et al. (2013) that relied on the Bullfrog cosmogenic age of 1.5 Ma to propose that incision rates above the knickzone were substantially lower than below the knickzone in Grand Canyon.

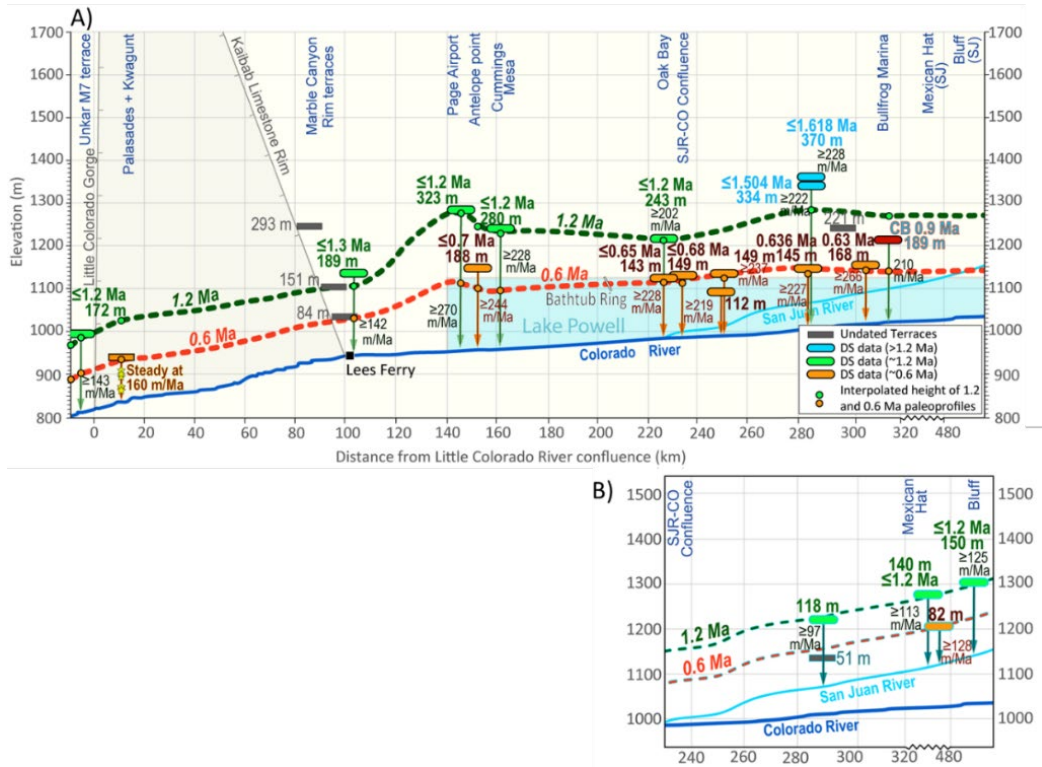


Figure 12 – A) Colorado and B) San Juan River pre-dam river profiles (Birdseye et al., 1922) showing terrace heights and locations. Blue (~ 1.6 Ma), green (~ 1.2 Ma) and orange (~ 0.6 Ma) rectangles are dated Colorado River terraces, with height (m), age (Ma) and incision rate (m/Ma), assuming MDAs approximate true depositional ages. The inset shows the same age terraces on the San Juan River with height (m), age (Ma), and incision rate (m/Ma). Grey rectangles are undated terraces. From left, new ages and incision rates for Unkar area terrace of ≤ 1.21 Ma yields ≥ 142 m/Ma -- similar to steady incision of 160 m/Ma documented in Palisades and Kwagunt areas using strath-to-strath regression (strath heights at Palisades and Kwagunt indicated by yellow stars on orange incision arrow; Crow et al., 2014). Lees Ferry terraces are from Pederson et al. (2013) and Billingsley and Priest (2013). N-dipping Kaibab limestone (line with ticks, highly vertically exaggerated) emerges at Lees Ferry and forms the rim of southward-deepening Marble Canyon that is overlain at various heights by undated terraces. Lake Powell terraces from this study suggest a zone of >230 m/Ma incision rates for Page Airport area terraces at 0.6 and 1.2 Ma, and a zone of >200 m/Ma terraces near San Juan confluence at 0.6 Ma. Upstream rates are still high for Bullfrog Marina at 210 m/Ma (189 m/0.9 Ma; Darling et al., 2012). B.) Incision rates up the San Juan river are lower at Big Bend (118 m/1.2 Ma), Mexican Hat (140 m/1.2 Ma and 82 m/0.64 Ma), and Bluff at 125 m/Ma (151 m/1.2 Ma; Heizler et al., 2021) emphasizing the anomalously high rates in the Lees Ferry knickzone and at the Colorado-San Juan River confluence.

Alternative models for the Lees Ferry knickzone

The major knickzone and convexity along the Colorado River profile at Lees Ferry at the head of Grand Canyon marks a major change in river gradient between the lower Colorado River and upper Colorado River basins. This knickzone has been variously interpreted as: 1) a transient knickzone left from the 5 Ma integration across the Grand Wash Cliffs (Pelletier, 2010); 2) a bedrock- influenced knickpoint located at the upper contact of the resistant Kaibab Limestone (Cook et al., 2005; Pederson et al., 2013); and/or 3) a steady state knickzone related to mantle-driven uplift (Crow et al., 2014). Figure 13 evaluates our new paleoprofile data in the context of these different models and illustrates how measuring long term incision rates from high terraces can help resolve debates about its origin.

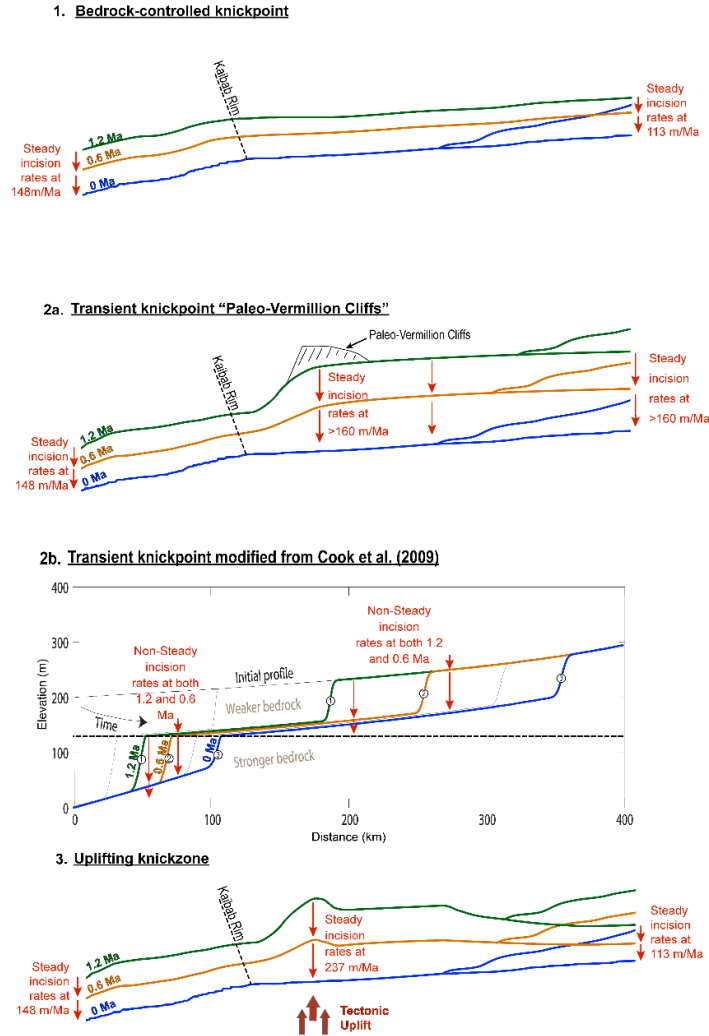


Figure 13 - Alternative hypotheses for Lees Ferry knickzone, given evidence for steady incision at 160 m/Ma downstream (RM 57) and 125 m/Ma upstream. 1) A bedrock controlled knickpoint would be fixed at the Kaibab Limestone contact, with faster steady incision below and slower above, resulting in parallel paleoprofiles above and below this contact and a slow upstream knickpoint migration of a few km/Ma. 2) A knickzone transient with higher incision rates near it focused because of either: 2A) pre-integration paleogeography such as a paleo Vermillion cliffs as suggested by the thermochronology data; or 2B) a wave of incision that moves the knickpoint from position 1 to 2 to 3, perhaps instigated by Colorado River integration across the Grand Wash cliffs (Cook et al., 2005) or from the edge of East Kaibab paleocanyon, but our data would require such a transient knickpoint to have passed RM 57 before 1.6 Ma to 2.68 Ma (the latter based on the speleothem data). 3) Uplift of the knickzone region would predict warping of paleoprofiles and resulting accelerated steady incision in the uplifting region.

Higher rates below than above the knickpoint (Figure 13, # 1) would be consistent with the steeper river gradient below than above the knickzone and the notion that the knickzone and double-concave profile of the greater Colorado River results from downstream baselevel fall due to integration of the Colorado River system to the Gulf of California. In this model, Grand Canyon and downstream reaches are responding to this lowered baselevel, whereas the shallower river gradient and slower incision upstream of the knickpoint reflect older landscapes that have not yet seen the lowered baselevel. Pelletier (2010) modelled the late Cenozoic geomorphic evolution of the Grand Canyon and suggested that migration of a knickpoint from Grand Wash fault to Lees Ferry would be compatible with stream power laws and with a ~6 Ma Grand Canyon. His geomorphic model was similar for either headward erosion or lake spill-over as the primary integration mechanism. The model suggests an eastward-propagating knickpoint with a velocity of ~100 km/Ma that resulted in rapid incision from westward Grand Canyon down to the level of the Redwall Limestone from 6 to 4 Ma and eastern Grand and Marble Canyons from 4 to 2 Ma, triggering a flexural-isostatic rebound of up to 350 m from the widening of the Grand Canyon. However, this hypothesis fails to explain the observed semi-steady incision rates in several reaches over the past 4 Ma (Crow et al., 2014) and now also fails to explain the higher incision rates of > 237 m/Ma within the knickzone region above Glen Canyon Dam (Figure 12).

Cook et al. (2009) described the Lees Ferry knickpoint as a bed-rock influenced transient and postulated a young pulse of rapid incision that is interacting with an upstream-dipping knickpoint localized at the resistant Kaibab Limestone (Figure 13, #2b). Their analysis suggested that a late pulse of rapid incision (for example during the past ~500 ka in

their model) is observed upstream of the Grand Canyon based on the postulated high rates reported by Marchetti and Cerling (2005), Cook et al. (2009), and Pederson et al. (2013) for areas upstream in the vicinity of the Henry Mountains. Such high incision above the knickzone, assuming it is not due to dating methods that produce minimum ages and hence maximum rates (e.g. Karlstrom et al., 2013), was postulated to be related to the relatively soft rocks above the knickpoint through which the incision wave could propagate while still being hung up at the Kaibab contact. This hypothesis predicts non-steady incision as the wave passes a given reach (Cook et al., 2009; their Fig. 12) and seems incompatible with observed semi-steady incision that suggests that any major transient knickpoint migration could not have passed through western Grand Canyon after 4 Ma, through eastern Grand Canyon after 1.2- 2.68 Ma, or through Glen Canyon in the past 1.6 Ma. The postulated strong bedrock influence is also generally incompatible with steady rates through time in all reaches measured so far regardless of the variations of bedrock strengths the river has incised through in each reach over the past several million years (Crow et al., 2014).

Cook et al. (2009) noted down-turned tributary profiles near their confluence with the Colorado River (e.g. the Little Colorado River), where the over steepened reaches imply 150-200 m elevation drops that may reflect a pulse of young increased incision due to knickpoint transience. The region outlined by down-turned profiles below tributary knickpoints identified by Cook et al. (2009, Fig. 1) coincides in part with areas where we document higher, but semi-steady, incision rates over the past 1.6 Ma. Models #2a and #3 in Figure 13 try to reconcile existing steady incision with limited transience of the Lees Ferry and Little Colorado River knickzones (e.g. Karlstrom et al., 2017). Figure 13 #2a shows one possibility suggested by the thermochronologic data (Figure 2), that there was a paleo-Vermillion cliffs

at 5 Ma that was eroded in the past 5 Ma after integration of the San Juan to the Colorado River such that isostatic rebound from differential erosion might add to downstream incision magnitudes and rates (Lazear et al., 2013; Pederson et al., 2013). However, based on present thermochronology data, it appears that the ~2 km magnitude of post-5 Ma denudation was similar from Lees Ferry to the San Juan headwaters such that this model has difficulty explaining the lower incision rates in the San Juan River near Mexican Hat and Bluff relative to higher rates both upstream in the San Juan Mountains and downstream in eastern Grand Canyon.

Our preferred model is shown in #3 of Figure 13 where the high incision rates in Glen Canyon are explained by a pulse of young tectonic uplift that has warped 0.6 and 1.2 Ma paleoprofiles along the Colorado River in the region between Lees Ferry and upper Lake Powell. This region agrees reasonably well with the region of rapid young incision suggested by the profile analysis of Cook et al (2009) and provides a tectonic mechanism to explain the observed steady average differential incision. The wavelength of the proposed flexure with an amplitude of ~100 m/Ma over a lateral distance of >200 km as seen in the reconstructed paleoprofiles from incision rates is reasonable for an elastic thickness of 30 km, as shown by isostatic modeling (Lazear et al., 2013). The lower rates of 113 m/Ma on the San Juan, in the Mexican Hat to Bluff areas above the downturn in its profile, is possibly explained in terms of the San Juan not yet being influenced by the lowered base level and young uplift that is affecting the Colorado River. Similarly, post-5 Ma incision rates on the Little Colorado River above its knickpoint have been steady at about 40 m/Ma (Karlstrom et al., 2017, their Fig. 14).

Evaluating mantle-driven uplift

Based on thermochronologic data (Hoffman, 2009; Mckeeon, 2009; Lee et al., 2012; Kelley and Karlstrom, 2017), we estimate that “ground zero” for the San Juan River and its confluence with the Colorado River at ~ 5 Ma was approximately 2 km higher in the stratigraphic section than today. Erosion of this thickness of strata in the past 5 Ma suggest an average denudation rates of ~2 km in 5 Ma or 400 m/Ma. Our measured minimum incision rates over the past ~0.6 and ~1.2 Ma are less than half of this suggesting faster denudation in the first 3 Ma following integration. But in the past 2 Ma, highest incision rates (~ 237 m/Ma) are observed in western San Juan headwaters and Glen Canyon, slowest (~113 m/Ma) in reaches across the Colorado Plateau, and intermediate (~148 m/Ma) in eastern Grand Canyon. As mentioned above, the differential rates suggest the possibility of differential tectonic uplift resulting in higher incision rates in and above the regionally important Lees Ferry knickzone, and in upstream diverging terraces in the San Juan headwaters.

Alternative, non-tectonic, hypotheses for differential incision of the Colorado and San Juan River system emphasize the geomorphic (and potential climatic; Chapin et al., 2008) forcings of regional river integration acting on a previously uplifted region. In these models, downward river integration through Grand Canyon at 5-6 Ma, from a base level of the Colorado Plateau to sea level, may explain the differential incision (Pederson et al., 2013). As discussed above, regional climate change influences such as onset of the southwestern monsoons due to opening of the Gulf of California ~ 6 Ma (Chapin et al., 2008) are possible explanations for initiation of integration, and increased glacial-interglacial cycles and change

to a regime of terrace flight deposition after ~ 2 Ma is also possible (Aslan et al., 2019). But our terrace record that goes back nearly ~ 2 Ma does not reveal non-steady incision in any reach that could be attributed to climate fluctuations.

Figure 14 plots incision rates along the Colorado-San Juan river above a deep mantle cross section showing P-wave velocities. The Colorado Rocky Mountains Experiment and Seismic Transect (CREST) showed that the lowest V_p and V_s velocities spanning the Colorado Rocky Mountain region are found beneath the San Juan Mountains. This area has the region's highest topography and its thinnest crust, suggestive of a rootless southern Rocky Mountain region with high topography supported, perhaps equally, by low-density crust and low-density mantle (Hansen et al., 2013). A sharp velocity contrast occurs between the San Juan headwaters and Farmington, NM that may help explain the differential incision via headwater uplift. Additionally, young (4 -7 Ma) magmatism took place in the western San Juan Mountains (Gonzales, 2015; 2017) that may have contributed to differential uplift. Thus, the previously published notions of a correlation between incision rate and underlying mantle velocity domains may apply for the San Juan to Colorado Plateau transition whereby heat and mass transfer across this deep-seated "edge" of the Colorado Plateau's lithosphere may be driving differential uplift (Karlstrom et al., 2012; MaCarthy et al., 2014; Hansen et al., 2013; Rosenburg et al., 2014; Nereson et al., 2013).

A sharp mantle velocity contrast is also found beneath the Lees Ferry region between higher velocity mantle in the core of the Colorado Plateau and lower velocities around the rims (Crow et al., 2014). In this case, high incision rates are seen in the zone of highest velocity gradient (gray bar in Fig. 14), but they persist on the Colorado River well above the

area of the mantle velocity transition into a region underlain by high velocity mantle. In contrast, rates are lower above the high velocity mantle along the San Juan River. Thus, our new data make this hypothesis unconvincing for the Colorado River across the Lees Ferry knickzone and may suggest more complex forcings.

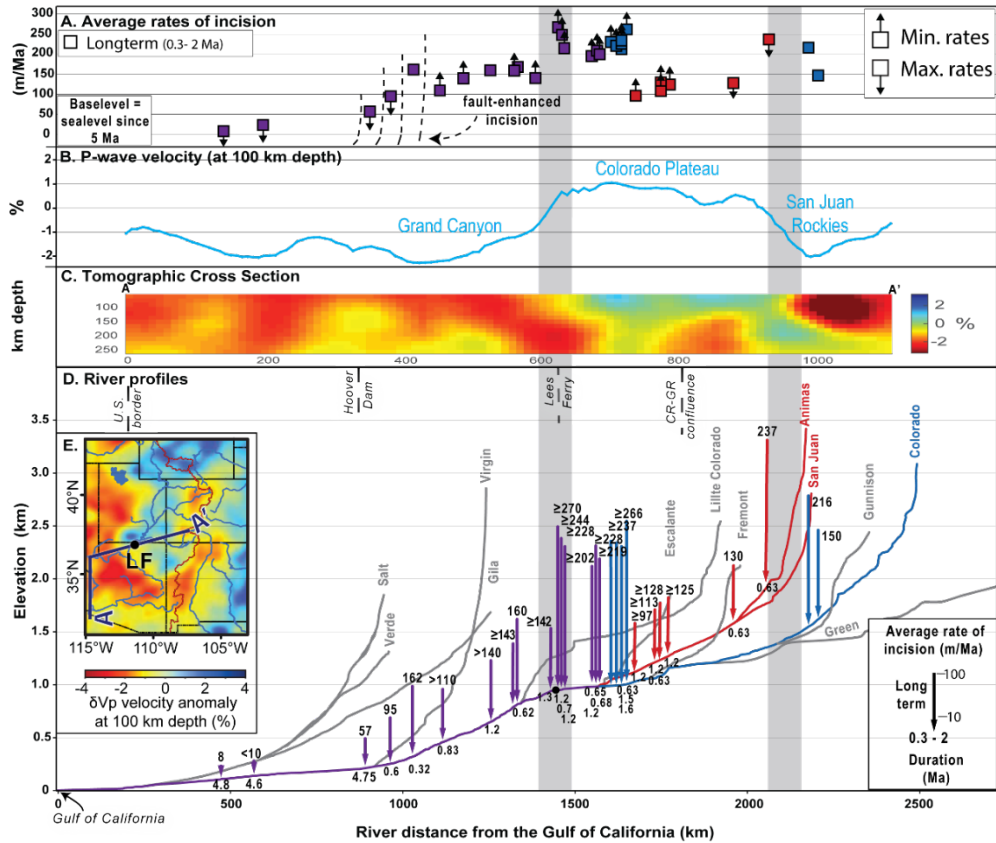


Figure 14 - A) Compiled average long-term incision rate data from the lower Colorado River up to the Animas River. Blue squares indicate long-term incision rates over 0.3 – 2 Ma. B) P-wave velocity at 100 km depth below Colorado and San Juan Rivers. C) P-wave tomographic cross sections beneath the river profiles along the Colorado and San Juan River (Brandon Schmandt, unpublished tomography). D) Colorado and San Juan river profiles derived from U.S. Geological Survey 90m DEM and Birdseye (1922); long-term incision rates at terrace locations along the Colorado and San Juan river profiles are color coded: purple and blue- Colorado River below and above, respectively, the San Juan confluence; red- San Juan River. Grey bars indicate zones of high mantle gradient at Lees Ferry and the Rocky Mountains. E) Inset map of P-wave velocity (Schmandt and Humphreys, 2010) showing velocity variation and the location of the river-subparallel tomographic cross sections in C).

Figure 15A explores the possibility that high incision rates above the Lees Ferry knickzone are a regional response of the disequilibrium Colorado River system to achieve an equilibrium concave-up profile by eliminating the regional concavity between Lees Ferry and the region of the Green-Colorado river confluence. This “geomorphic” explanation does not explain why the knickzone is there, or its time evolution, but considers an interaction of tectonic and geomorphic forcings. The observed higher steady incision above the bedrock knickzone at Lees Ferry as well as the anti-correlation, where shallower river gradients above and within the knickzone correspond to faster incision rates, are both unexpected from knickpoint transience but might be expected across an uplifting 1000-km-wide convexity.

Figure 15B shows our model where plateau-like uplift of the San Juan headwaters relative to Colorado Plateau, and of the western Colorado Plateau relative to sea level are interpreted to concentrate incision at the edges of the uplifting plateau-like blocks. In the case of the Lees Ferry area, the 30 km-thick elastic plate results in a broad convexity formed above the zone of mantle upwelling and increased lithospheric buoyancy. The youthfulness of 5 Ma integration is such that lower base level (at sea level) is not yet “felt” by upstream reaches well above the Lees Ferry and in tributaries that cross the core of the Colorado Plateau. This process of epeirogenic plateau uplift and incision at the edges is ongoing in many orogens such as Tibet (e.g. Lu et al., 2004) and the Andes (e.g. Schildgen et al., 2007) and involves complex feedback between tectonic, geomorphic, and climate forcings.

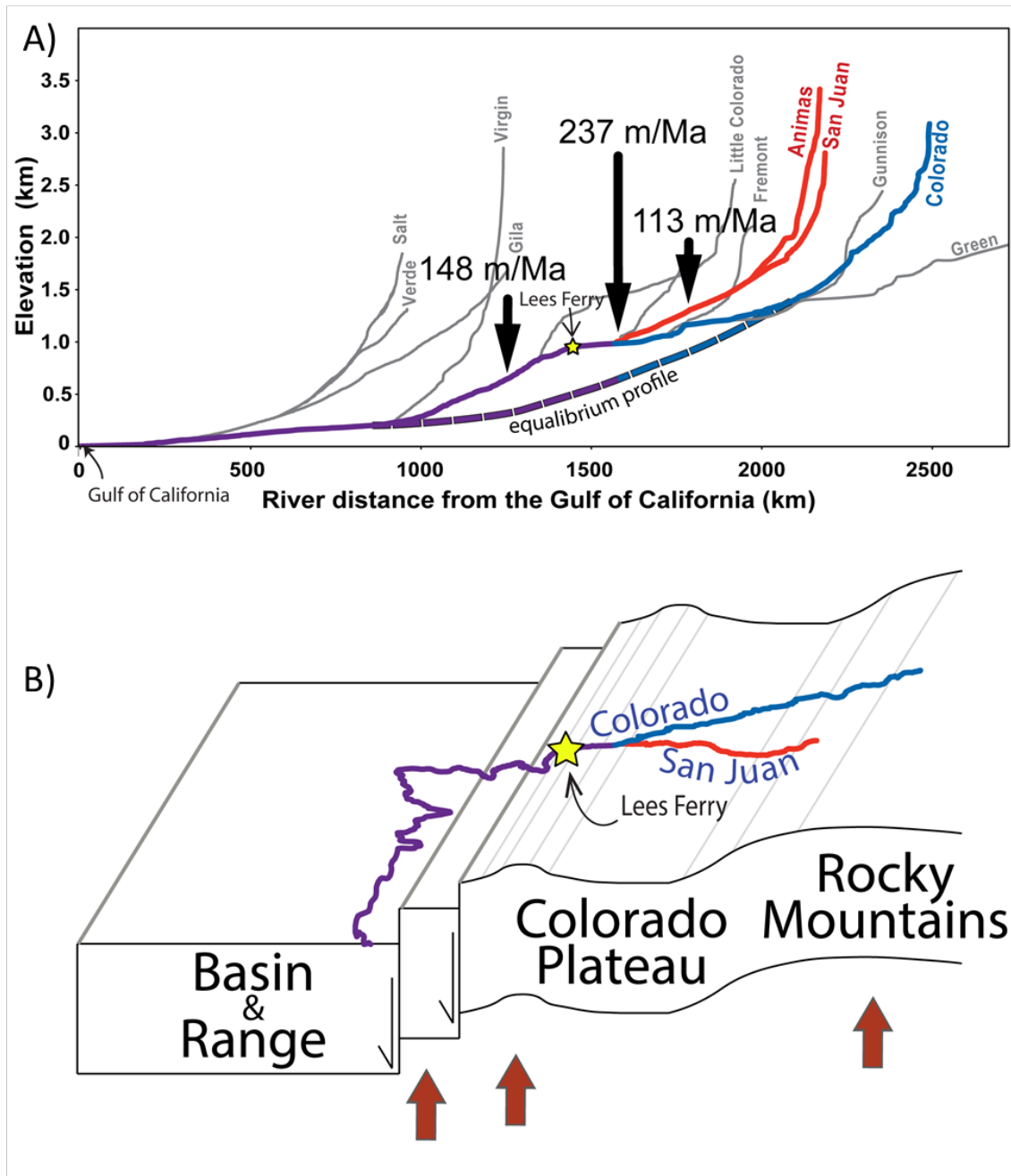


Figure 15 – Differential uplift interpretation for the Colorado-San Juan river system. A) The observed increased incision rates in the wide region above the Lees Ferry knickzone is interpreted as the response of the Colorado River to achieve an equilibrium concave-up profile (dashed purple and blue line). B) Plateau-like uplift of the San Juan headwaters relative to Colorado Plateau, and Lees Ferry region relative to Grand Canyon are interpreted to concentrate incision at the edges of the uplifting edges of the Colorado Plateau.

CONCLUSIONS

Analyses of terrace ages help to correlate terraces along the continental-scale Colorado and San Juan river system and suggest markedly different incision rates in different reaches. These contribute to the understanding about what is driving incision and landscape evolution in the Rocky Mountain-Colorado Plateau region. Thermochronology studies in the lower, middle, and upper San Juan River suggest a young (5 Ma) river, showing ~2 km of exhumation (leading to an additional ~1 km of isostatic uplift) in the past 5 Ma for the region from Lees Ferry to the San Juan Mountains. Two major age populations for terraces along the study area have been observed at ~1.2 Ma and ~0.6 Ma. The 0.6 Ma terraces are approximately half as high above the modern rivers as the 1.2 Ma terraces in all reaches, but terrace heights vary from reach to reach. This emphasizes that solely using terrace height for terrace correlation across the Colorado-San Juan river system would be incorrect. Relative to river level, in eastern Grand Canyon to Lees Ferry, incision rates have been semi-steady at ≥ 142 m/Ma since 1.2 Ma and 160 m/Ma since 0.623 Ma (Crow et al., 2014). Incision rates just above the Lees Ferry knickpoint are much higher, ≥ 237 m/Ma over the past 1.2 Ma and ≥ 200 m/Ma over the past 0.630 Ma near the San Juan-Colorado River confluence (Heizler et al., 2021). These high incision rates continue up the Colorado River at least as far as Bullfrog Marina. In contrast, incision rates on the San Juan River as it crosses the interior of the Colorado Plateau are lower but still steady at about 113 m/Ma over the past ca. 1.2 Ma. In the uppermost reaches of the San Juan system, along the Animas River, incision has been steady at 237 m/Ma over the past 0.630 Ma and terraces converge downstream towards Farmington, NM. Across the Lees Ferry knickzone, the observed differential, but everywhere steady, incision is acting to reduce the disequilibrium convexity of the entire Colorado River system

“double concave” profile. This regional convexity occurs above a zone of sharp contrast in mantle velocity (cf. Schmandt and Humphreys, 2010). Similarly, a transition in incision rates in the San Juan River headwaters also occurs across a marked change in mantle velocity. The provocative implication is that the cause of the observed differential incision over the million-year timeframe may be related to upwellings of low velocity mantle beneath the margins of the Colorado Plateau relative to high velocity mantle in its interior. This differential rate of ~ 100 m/Ma implies ~ 500 m of uplift of the Rockies relative to the Colorado Plateau over the past 5 Ma. Simultaneously, based on ~ 700 m/Ma of differential incision through Grand Canyon (Crow et al., 2014), the change across the Lees Ferry knickzone of ~ 100 m/Ma (500 m) adds to an overall uplift of the Glen Canyon region of ~ 1.2 km relative to sea level in the past 5 Ma.

DATA REPOSITORY

List of Data Repository Materials

Data Tables

DR Table 1. Terrace correlation to accompany Figure 3

Photos of dated terraces

P-25

P-7

P-24 and P-32

P-14

P-26

P-18

SJR-2

A-4

A-6

Bullfrog Terrace

Data Tables

DR Table 1

Area Name	This Study	Published terrace numbering	Map name (working column)	Location	sample name	Latitude	Longitude	strath height ARL(m)	dated age (Ma)	uncertainty (Ma)	estimated age (Ma)	dating method	incision rate (m/ka)	
Colorado R. Eastern Grand Canyon	C9	M7 ²		Unkar terrace below basalt canyon	K17-73			183 (172 - 183)	1.21	0.03	±1.21	DS	±143	
	C8	M6 ²		Eastern GC				133 (120 - 133)						
	C7	M5 ²		Palasades	RC10-PAL-28	36.14314	-111.8116	94 (85-94)	0.623	0.182 / - 0.078	0.623	U/Th	160	
	C4	M4 ¹		Eastern GC				52						
	C3	M3 ¹		Eastern GC				38						
C1	M1 ¹		Eastern GC				8							
Colorado R. Lees Ferry	C9	M9 ² ; Qg10 ²⁻⁴ ; Qg11 ²⁻⁴		Johnson Mesa	K16-MAR-3	36.86211	-111.61338	189 (189-192)	1.329	0.009	±1.329	DS	±142	
	C8	M8 ² ; Qg9 ²⁻⁴		Navajo Bridge				169 (151-169)						
	C7	M7 ² ; Qg8 ²⁻⁴		Lower Johnson point				115 (88-115)						
	C7(7);C6	M6 ² ; Qg6 ²⁻⁴ ; Qg7 ²⁻⁴		Cathedral Meah				51 (84-91)						
	C5	M5 ² ; Qg5 ²⁻⁴		Pania Canyon				39 (33-39)						
	C4	M4 ² ; Qg4 ²⁻⁴		Ranger Station				39 (27-39)						
	C3	M3 ² ; Qg3 ²⁻⁴		Lees Ferry gravels				23 (14-23)						
	C2	M2 ² ; Qg2 ²⁻⁴		Upper Ferry				14 (8-14)						
	C1	M1 ² ; Qg1 ²⁻⁴		Lower Ferry				5 (2-5)						
	Lower Little Colorado R.	LCR9	7 ³		Butte fault cave RMS7		36.1271	-111.8223	445	2.68	Large	2.68	U-Pb	166
LCR8		7 ³		Crooked Ridge		36.3576	-111.3788	425 (375-425)	2	0.02	2	DS		
LCR7(7)		6 ³		Prominent terrace of Colley 1969		35.669359	-111.34972	172	0.89	0.02	0.89	Ar-Ar	159	
LCR6		5 ³		Black point Basalt flow				117						
LCR5		5 ³		Prominent Colley terrace				76						
LCR4		4 ³		Cooley terrace 5				53						
LCR3		3 ³		Cooley terrace 4; Tappen flow		35.881296	-111.442331	53	0.34	0.006	0.34	Ar-Ar	156	
LCR2		2 ³		Cooley terrace 3				27						
LCR1		1 ³		Cooley terrace 2				15						
LCR1		1 ³		Cooley terrace 1				9						
Colorado R. Marble/Glen Canyon	C9	Qg14 ⁴		Paige Airport	K17-POW-18	36.93373	-111.44632	325 (347-367)	±1.08	0.04	1.2	DS	±300	
	C9	Qg13 ⁴		Waheep Bay				311 (323-331)						
	C9	Qg14 ⁴		Cummings Mesa	K20-POW-26	36.92444	-111.39019	280 (302-305)	±1.23	0.02	±1.2	DS	±228	
	C9	Qg15 ⁴		Waheep Bay				299 (293-299)						
	C8	Qg14 ⁴		Waheep Bay				280 (274-280)						
	C8	Qg13 ⁴		Waheep Bay				262 (244-262)						
	C8	Qg12 ⁴		Waheep Bay				244 (232-244)						
	C7	Qg11 ⁴		Antelope Point	GLG-CT	36.965	-111.436	188 (185-192)	0.77	0.04	±0.77	DS	±244	
	C7(7)	Qg10 ⁴		Antelope Point				189 (183-189)						
	C7(7)	Qg9 ⁴		Ferry Swale				194 (189-194)						
San Juan Colorado R. confluence	C9			Cha Surface 4103'	K20-POW-34; K21-POW-32a	37.118993	-110.98358	243	1.24	0.03	±1.24	DS	±202	
	C8			Oak Island	K17-POW-7a	37.12543	-110.95264	189						
	C7			Hidden Passage	K17-POW-14	37.18824	-110.93148	149	0.679	0.006	±0.679	DS	±219	
	C7			Low Oak Bay	K20-POW-25	37.11611	-110.95922	143	0.627	0.012	±0.627	DS	±228	
	SJR7	Gate ⁸		Bigbend #1	K21-POW-29	37.26361	-110.69614	118	1.221	0.019	±1.221	DS	±97	
	SJR7	Gate ⁸		Bigbend #2	K21-POW-30	37.26489	-110.69668	98						
	SJR5	Gate ⁸		Bigbend #3	K21-POW-31	37.26667	-110.70048	51						
	Colorado R. above SJR to Bullfrog	C13	Qat ¹		Annie's Canyon High #1	K21-POW-35	37.36657	-110.74377	370	1.618	0.01	±1.618	DS	±238
		C13	Qat ¹		Annie's Canyon High #2	K21-POW-36	37.38925	-110.74156	358					
		C12	Qat ¹		Annie's Canyon High #3	K21-POW-37	37.3712	-110.74116	334	1.504	0.015	±1.504	DS	±222
C9				Lake Canyon High	K21-POW-39	37.43126	-110.7139	221						
C9				Bullfrog	Darling et al., 2012	37.52	-110.7	180	0.9	0.13	1.5	Isochron Cosmo Burial	210	
C9				Bullfrog	K21-POW-40	37.48172	-110.74104	183						
C9				Bullfrog	K21-POW-41	37.47029	-110.72921	168	0.63	0.03	±0.63	DS	±286	
C8		Gate ⁸		Annie's Canyon Low	K21-POW-28	37.25056	-110.73051	145	0.636	0.006	±0.636	DS	±227	
C8				Hole in the wall high	K21-POW-34	37.25084	-110.86099	149	0.628	0.005	±0.628	DS	±237	
C7				Hole in the wall Low	K21-POW-33	37.24754	-110.8833	112	0.662	0.012	±0.662	DS	±264	
C7			Lake Canyon Low	K21-POW-38	37.43119	-110.70229	116							
San Juan R. Mexican Hat to Bluff	SJR9			Bluff	SJR 0205-2	37.2982	-109.54904	151	1.208	0.008	±1.2	DS	±125	
	SJR9			Mexican Hat High	SJR21-MH-1	37.15945	-109.8114	140	1.236	0.016	±1.236	DS	±113	
	SJR7			Mexican Hat Low	SJR21-MH-3	37.15357	-109.8621	82	0.64	0.04	±0.64	DS	±128	
San Juan-Animas confluence Farmington	A9(7)	t2h ⁸		Farmington Area	MA20-ANI-3	36.78032	-108.17783	188 (180-188)						
	A9(7)	t2i ⁸		Farmington Area	MA20-ANI-2	36.77854	-108.1874	187 (177 - 187)						
	A8	t2 ⁸		Farmington Area	MA20-ANI-1	36.75629	-108.09147	115 (110-119)						
	A7	t4ab ⁸		Farmington Area				83 (77-83)			0.630	overlain by Lava C B	130	
	A5	t5 ⁸		Farmington Area				40 (37-40)						
	A3	t6 ⁸		Farmington Area				28 (16-28)						
	A2	t7 ⁸		Farmington Area				15 (3-15)						
	Animas R. Cedar Hill	A13(7)	t1 ⁸		Slane Knob	MA20-ANI-4	36.82319	-107.86655	411 (341-411)					
		A12(7)	t2 ⁸		Cedar Hill Area				352					
		A12(7)	t3 ⁸		Cedar Hill Area	MA20-ANI-7	36.95284	-107.85284	339					
A11(7)		t2 ⁸		Cedar Hill Area				315						
A11(7)		t2u ⁸		Cedar Hill Area	MA20-ANI-8	36.95568	-107.86438	302						
A11(7)		t2e ⁸		Cedar Hill Area				299 (296-299)						
A10(7)		t2f ⁸		Cedar Hill Area	MA20-ANI-5	36.9827	-107.89297	257 (254-257)						
A9(7)		t2g ⁸		Cedar Hill Area				229 (225-229)						
A9(7)		t2h ⁸		Cedar Hill Area				210 (7)						
A7		t4ab ⁸		Cedar Hill Area; Arch Rock Canyon	MA20-ANI-6	36.87979	-107.86161	110 (95-110)			0.630	overlain by Lava C B	170	
Animas R. Florida Mesa	A5	t5a ⁸		Cedar Hill Area				67						
	A3	t6 ⁸		Cedar Hill Area				39 (24-39)						
	A2	t7 ⁸		Cedar Hill Area				12 (3-12)						
	A9(7)	t2g ⁸ ; A ¹		Florida Mesa Area				250 (7)						
	A7	t4a ⁸		Florida Mesa Area				153 (141-153)			0.630	overlain by Lava C B	242	
	A6	t4b ⁸		Florida Mesa Area				131 (128-131)			0.630	overlain by Lava C B	207	
	A6	t4c ⁸		Florida Mesa Area				124 (117-124)						
	A6	t4d ⁸		Florida Mesa Area				112 (109-112)						
	A5	t4e ⁸		Florida Mesa Area				93 (87-93)						
	A5	t4b ⁸		Florida Mesa Area				86 (83-86)						
A5	t4c ⁸		Florida Mesa Area				76 (73-76)							
A5	t4d ⁸		Florida Mesa Area				70							
A5	t4e ⁸		Florida Mesa Area				71 (65-71)							
A3	t6 ⁸		Florida Mesa Area				29 (22-29)							
A2	t7 ⁸		Florida Mesa Area				6 (3-6)							

Photos of Dated Terraces

P-25



Photos by Laura Crossey



Sample ID	Age (Ma)	Latitude	Longitude	Elevation (meters)	Strath Height Above River (meters)
P-25	$\leq 0.627 \pm 0.012$	37.11611	-110.95922	1105	143

P-7

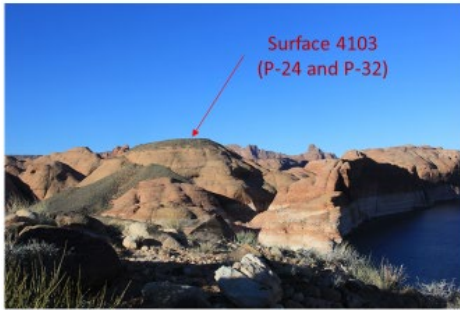


Photos by Laura Crossey



Sample ID	Age (Ma)	Latitude	Longitude	Elevation (meters)	Strath Height Above River (meters)
K17-POW-7	≤ 10	37.12543	-110.9529	1142	199

P-24 and P-32



Photos by Laura Crossey

Sample ID	Age (Ma)	Latitude	Longitude	Elevation (meters)	Strath Height Above River (meters)
P-24 and P-32	1.237±0.034	37.19690	-110.89388	1200	243

P-14



Photo by Laura Crossey

Sample ID	Age (Ma)	Latitude	Longitude	Elevation (meters)	Strath Height Above River (meters)
P-14	≤0.679±0.006	37.16824	-110.9315	1132	149

P-26



Sample ID	Age (Ma)	Latitude	Longitude	Elevation (meters)	Strath Height Above River (meters)
P-26	$\leq 1.232 \pm 0.016$	36.99244	-111.39019	1246	280



P-18



Photos by Laura Crossey

Sample ID	Age (Ma)	Latitude	Longitude	Elevation (meters)	Strath Height Above River (meters)
P-18	$\leq 1.203 \pm 0.036$	36.93373	-111.4463	1282	325

SJR-2



Bluff quarry – Photo by Laura Crossey

Sample ID	Age (Ma)	Latitude	Longitude	Elevation (meters)	Strath Height Above River (meters)
SJR-2	$\leq 1.208 \pm 0.008$	37.2982	-109.549	1453	151



Bluff Terrace – SJR-2 sample pit photo by Mary Gillam

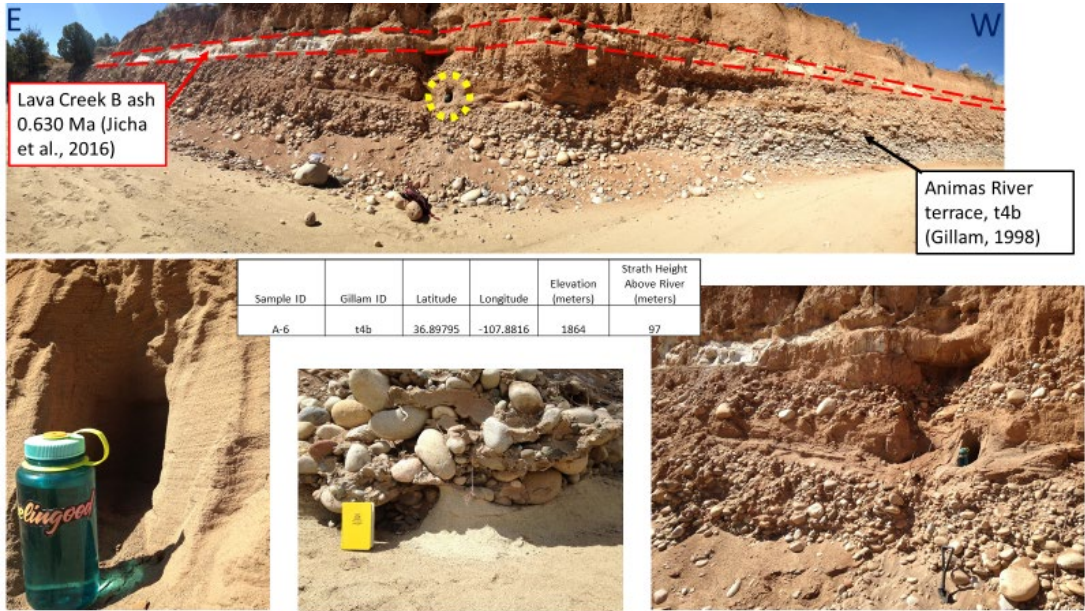
A-4



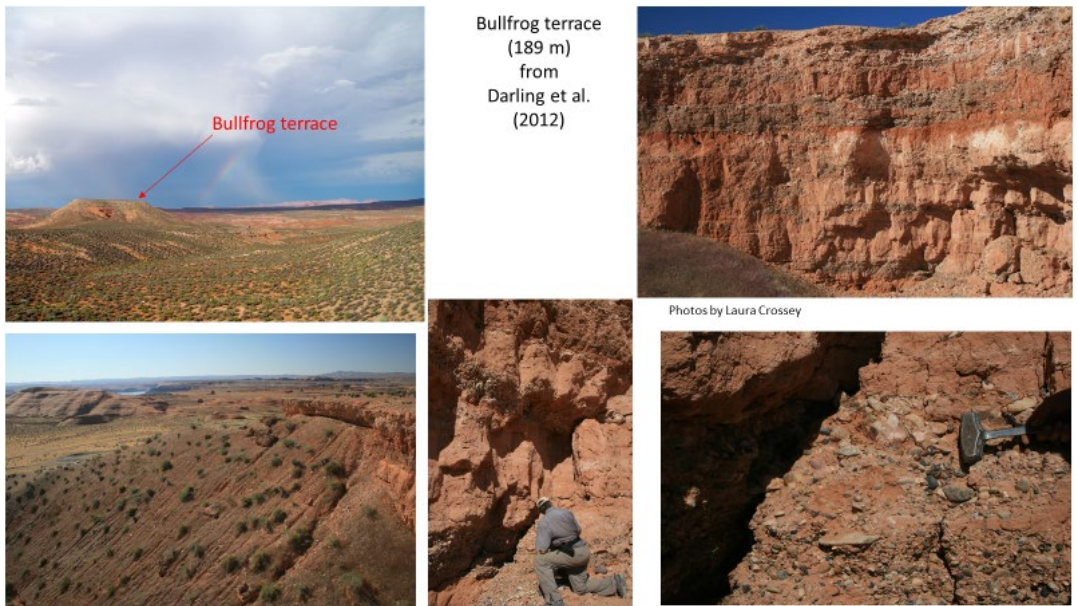
Sample ID	Gillam ID	Latitude	Longitude	Elevation (meters)	Strath Height Above River (meters)
A-4	t1u	36.82319	-107.8666	2081	334



A-6



Bullfrog Terrace



REFERENCES CITED

Antoine, P., Lozouet, N.L., Chausse, C., Lautridou, J.P., Pastre, J.F., Auguste, P., Bahain, J.J., Falgueres, C., Galehb, B., 2007, Pleistocene fluvial terraces from northern France (Seine, Yonne, Somme): synthesis, and new results from interglacial deposits: *Quaternary Sciences Review*, v. 26, p. 2701-2723.

Aslan, A., Karlstrom, K., Hood, W.C., Cole, R.D., Oesleby, T.W., Betton, C., Sandoval, M.M., Darling, A., Kelley, S., Hudson, A., Kaproth, B., Schoepfer, S., Benage, M., Landman, R., 2008, River incision histories of the Black Canyon of the Gunnison and Unaweep Canyon: Interplay between late Cenozoic tectonism, climate change, and drainage integration in the western Rocky Mountains: *Geological Society of America Field Guide 10*, p. 175–202.

Aslan, A., Heizler, M.T., Karlstrom, K.E., Granger, D.E., Martin, E., 2019. Detrital sanidine and cosmogenic burial age constraints support post-2 Ma integration of the upper Green River across the Uinta Mountains. *Geological Society of America, Abstracts with Program*, v. 51, no. 7.

Aslan, A., Karlstrom, K.E., Kirby, E., Heizler, M.T., Granger, D.E., Feathers, J.K., Hanson, P.R. and Mahan, S.A., 2019, Resolving time-space histories of Late Cenozoic bedrock incision along the Upper Colorado River, USA: *Geomorphology*, v. 347, p.106855.

Babenroth, D.L., Strahler, A.N., 1945, Geomorphology and structure of the East Kaibab monocline, Arizona and Utah: *Geological society of America Bulletin*, v. 56, p. 107-150.

Billingsley G.H. Priest S.S., 2013, Geologic map of the Glen Canyon Dam 30' × 60' quadrangle, Coconino County, northern Arizona: U.S. Geological Survey Scientific Investigations Map 3268, scale 1:50,000, 39 p.

Birdseye, C.H., Gerdine, T.G., and Chenoweth, W.R., 1922, Plan and profile of the Colorado River, Lees Ferry, Arizona, to mouth of Green River, Utah: San Juan River mouth to Chinle Creek, Utah, and certain tributaries: U.S. Geological Survey topographic, 1 map, 22 sheets, 1:31, 680.

Bridgland, D., and Westaway, R., 2008, Climatically controlled river terrace staircase: A worldwide Quaternary phenomenon: *Geomorphology*, v. 98, p. 285-315.

Cather, S.M., Connell, S.D., Chamberlin, R.M., McIntosh, W.C., Jones, G.E., Potochnik, A.R., Lucas, S.G., and Johnson, P.S., 2008, The Chuska erg: Paleogeomorphic and paleoclimatic implications of an Oligocene sand sea on the Colorado Plateau: *Geological Society of America Bulletin*, v. 120, p. 13–33.

Condie, K.C., 1964, Crystallization of syenite porphyry from Navajo Mountain, southern Utah: *Geological Society of America Bulletin*, v. 75, p. 359–362.

Cook, K.L., Whipple K.X., Heimsath, A.M., Hanks, T.C., 2009, Rapid Incision of the Colorado River in Glen Canyon – Insights from channel profiles, local incision rates, and modeling of lithologic controls: *Earth Surf. Process. Landforms*, v. 34, p. 994-1010.

Cooley, M.E., Davidson, E.S., 1963, The Mogollon Highlands – their influence on Mesozoic and Cenozoic erosion and sedimentation: *Arizona Geological Society Digest*, v. 6, p. 7-35.

Cross, W., and Larsen, E.S., 1935, A brief review of the geology of the San Juan region of southwestern Colorado: *U.S. Geological Survey Bulletin* 843, p. 138.

Crow, R., Karlstrom, K., Asmerom, Y., Schamndt, B., Polyak, V., and DuFrane, S.A., 2011, Shrinking of the Colorado Plateau via lithospheric mantle erosion: Evidence from Nd and Sr isotopes and geochronology of Neogene basalts: *Geology*, v. 39, p. 27–30.

Crow, R., Karlstrom, K., Darling, A., Crossey, L., Polyak, V., Granger, D., Asmerom Y., Schmandt, B., 2014, Steady incision of Grand Canyon at the million year timeframe: A case for mantle-driven differential uplift: *Earth and Planetary Science Letters*, v. 397, p. 159-173.

Crow, R.S., Schwing, J.E., Karlstrom, K.E., Heizler, M.T., Pearthree, P.A., House, P.K., Dunlin, S.A., Stelten, M.E., and Crossey, L.J., 2019b, Redefining the age of the Colorado River: *Geological Society of America Abstracts with Programs*, v. 51, no. 5.

Crow, R.S., Schwing, J., Karlstrom, K.E., Heizler, M., Pearthree, P.A., House, P.K., Dunlin, S., Janecke, S.U., Stelten, M., Crossey, L.J., 2021, Redefining the age of the lower Colorado River, southwestern United States: *Geology*, v. 49, p.

Darling, A.L., Karlstrom, K.E., Granger, D.E., Aslan, A., Kirby, E., Ouimet, W.B., Lazear, G.D., Coblenz, D.D., Cole, R.D., 2012, New incision rates along the Colorado River system based on cosmogenic burial dating of terraces: Implications for regional controls on Quaternary incision: *Gesphere*, v. 8, p. 1020-1041.

Deino, A., Potts, R., 1990, Single-Crystal $^{40}\text{Ar}/^{39}\text{Ar}$ Dating of the Olorgesailie Formation, Southern Kenya Rift, *Journal of Geophysical Research*, v. 95, p. 8453-8470.

Dethier, D.P., 2001, Pleistocene incision rates in the western United States calibrated using Lava Creek B tephra: *Geology*, v. 29, p. 783-786.

Demir, T., Seyrek, A., Westaway, R., Guillou, H., Scaillet, S., Beck, A., Bridgland, D.R., 2012, Late Cenozoic regional uplift and localized crustal deformation within the

northern Arabian Platform in Southeast Turkey: investigation of the Euphrates terrace staircase using multidisciplinary techniques: *Geomorphology*, v. 165-166, p. 7–24.

Dorsey, R.J., Fluette, A., McDougall, K., Housen, B.A., Janecke, S.U., Axen, G.J., and Shirvell, C.R., 2007, Chronology of Miocene–Pliocene deposits at Split Mountain Gorge, southern California: A record of regional tectonics and Colorado River evolution: *Geology*, v. 35, p. 57–60.

Garvin C.D., Hanks, T.C., Finkel, R.C., Heimsath, A.M., 2005, Episodic incision of the Colorado River in Glen Canyon, Utah: *Earth Surf. Process. Landforms*, v. 30, p. 973-984.

Gillam, M.L., 1998, Late Cenozoic geology and soils of the lower Animas River Valley, Colorado and New Mexico [Ph.D. Thesis] University of Colorado, 477 p.

Goff, F., 2010, The Valles Caldera: New Mexico's supervolcano: *New Mexico Earth Matters*, v. 10, p. 1-4.

Gonzales, D.A., 2017, A review and revision of late Mesozoic to Cenozoic pluton chronology in the Rico Mountains, southwestern Colorado, in Karlstrom, K.K., Gonzalez, D.A., Zimmerer, M.J., Heizler, M., and Ulmer-Scholle, D.S., eds., *Geology of the Ouray-Silverton Area: New Mexico Geological Society Guidebook 68*, p. 91–96.

Gonzales, D.A., 2015, New U-Pb zircon and $^{40}\text{Ar}/^{39}\text{Ar}$ age constraints on the Late Mesozoic to Cenozoic plutonic record in the Western San Juan Mountains: *The Mountain Geologist*, v. 52, p. 5–42.

Granger, D.E., 2006, A review of burial dating methods using ^{26}Al and ^{10}Be , in Alonzo-Zarza A.M. Tanner L.H., eds., *In Situ-Produced Cosmogenic Nuclides and*

Quantification of Geological Processes: Geological Society of America Special Paper, v. 415, p. 1-16.

Guido, Z.S., Ward, D.J., Anderson, R.S., 2007, Pacing the post-Last Glacial Maximum demise of the Animas valley glacier and the San Juan Mountain ice cap, Colorado: *Geology*, v. 35, p. 739-742.

Hansen S.M. Dueker K.G. Stachnik J.C. Aster R.C. Karlstrom K.E., 2013, A rootless Rockies—Support and lithospheric structure of the Colorado Rocky Mountains inferred from CREST and TA seismic data: *Geochemistry Geophysics Geosystems*, v. 14, p. 2670–2695.

Harvey, A.M., Wells, S.G., 1987, Response of Quaternary fluvial systems to differential epeirogenic uplift: Aguas and Feos river systems, southeast Spain: *Geology*, v. 15, p. 689-693.

Heizler, M.T., Karlstrom, K.E., Albonico, M., Hereford, R., Beard, S., Crossey, L., and Sundell, K., 2021, Detrital sanidine $^{40}\text{Ar}/^{39}\text{Ar}$ dating confirms < 2 Ma age of Crooked Ridge paleoriver and deep denudation of the southwestern Colorado Plateau, *Geosphere*, v. 17, p. 1-17

Hereford, R., Beard, L.S., Amoros, L., House, P.K., and Pecha, M., 2016, Reevaluation of the Crooked Ridge river – Early Pleistocene (ca. 2 Ma) age and origin of the White Mesa alluvium, northeast Arizona: *Geosphere*, v. 12, p 768-789.

Hildreth, W., 1979, The Bishop Tuff: evidence for the origin of compositional zonation in silicic magma chambers: Geological Society of America Special paper, v. 180, p. 43-76.

Hoffman, M.D., 2009, Mio-Pliocene erosional exhumation of the central Colorado Plateau, eastern Utah: New insights from apatite (U-TH)/He thermochronometry [M.S. Thesis] University of Kansas 176 p.

Hunt, C.B., 1969, Geologic history of the Colorado River, in the Colorado River region and John Wesley Powell: U.S. Geological Survey professional Paper 669, p. 59-130.

Izett, G.A., and Wilcox, R.E., 1982, Map showing localities and inferred distribution of the Huckleberry Ridge, Mesa Falls, and Lava Creek ash beds (Pearlette family ash beds) of Pliocene and Pleistocene age in the western United States and southern Canada: U.S. Geological Survey Miscellaneous Investigation Series Map I-1325, scale 1:4000000.

Jicha, B.R., Singer, B.S., Sobol, P., 2016, Re-evaluation of the $^{40}\text{Ar}/^{39}\text{Ar}$ sanidine standards and supereruptions in the western U.S. using Noblesse multi-collector mass spectrometer: *Chemical Geology*, v. 431, p.54-66.

Johnson, B., Gillam, M., Beeton, J., 2017, Glaciations of the San Juan Mountains: A review of work since Atwood and Mather: New Mexico geological society fall field conference guidebook - 68 The Geology of the Ouray-Silverton Area, p. 195-204.

Karlstrom, K., Darling, A., Crow, R., Lazear, G., Aslan, A., Granger, D., Kirby, E., Crossey, L., Whipple, K., 2013, Colorado River Chronostratigraphy at Lee's Ferry, Arizona, and the Colorado Plateau Bull's-eye of incision: *Comment: Geology*, v. 41, p. e303, doi:10.1130/G34550C.1

Karlstrom, K.E., Crow, R., Crossey, L.J., Coblenz, D., Van Wijk, J.W., 2008, Model for tectonically driven incision of the younger than 6 Ma Grand Canyon: *Geology*, v. 36, p. 835-838.

Karlstrom, K.E., Coblenz, D., Dueker, K., Ouimet, W., Kirby, E., Wijk, J.V., Schmandt, B., Kelley, S., Lazear, G., Crossey, L.J., Crow, R., Aslan, A., Darling, A., Aster, R., MacCarthy, J., Hansen, S.M., Stachnik, J., Stockli, D.F., Garcia, R.V., Hoffman, M., McKeon, R., Feldman, J., Heizler, M., Donahue, M.S., CREST working Group, 2012, Mantle-driven dynamic uplift of the Rocky Mountains and Colorado Plateau and its surface response: Toward a unified hypothesis: *Lithosphere*, v.4, p. 3-22.

Karlstrom, K.E., Crossey, L.J., Embid, E., Crow, R., Heizler, M., Herefor, R., Beard, L.S., Ricketts, J.W., Cather, S., Kelley, S., 2017, Cenozoic incision of the Little Colorado River: Its role in carving Grand Canyon and onset of rapid incision in the past ca. 2 Ma in the Colorado River System: *Geosphere*, v. 13, p. 49-81.

Kelley, S., Karlstrom, K.E., 2017, Thermal and structural history of Paleozoic and Proterozoic rocks in the vicinity of Molas Pass, northern Needle Mountains, southwestern Colorado: New Mexico geological society fall field conference guidebook - 68 The Geology of the Ouray-Silverton Area, p. 97-102.

Kuiper, K. F., Deino A., Hilgen, F. J., Krijgsman, W., Renne, P. R., and Wijbrans, J. R., 2008. Synchronizing the rock clocks of Earth history. *Science*, v. 320, p. 500–504.

Lazear, G., Karlstrom, K.E., Aslan, A., Kelley, S., 2013, Denudation and flexural isostatic response of the Colorado Plateau and southern Rocky Mountain region since 10 Ma: *Geosphere*, v. 9, p. 792–814.

Lee, J.P., Stockli D.F., S.A., Kelley, Pederson J.L., Karlstrom, K.E., Ehlers, T.A., 2012, New thermochronometric constraints on the Tertiary landscape evolution of the central and eastern Grand Canyon, Arizona: *Geosphere*, v. 9, p. 216-228.

Lucchitta, I., Holm, R.F., and Lucchitta, B.K., 2011, A Miocene River in northern Arizona and its implications for the Colorado River and Grand Canyon: *GSA Today*, v. 21, p. 4-10.

Lu, H.Y., Wang, X.Y., An, Z.S., Miao, X.D., Zhu, R.X., Ma, H.Z., Li, Z., Tan, H.B., Wang, X.Y., 2004, Geomorphic evidence of phased uplift of the northeastern Qinghai-Tibet Plateau since 14 million years ago: *Science in China*, v. 47, p. 822-833.

Lucchitta, I., Holm, R.F., and Lucchitta, B.K., 2013, Implications of the Miocene (?) Crooked Ridge river of northern Arizona for the evolution of the Colorado River and Grand Canyon: *Geosphere*, v. 9, p. 1417-1433.

Lucchitta, I., Holm, R., 2020, Re-evaluation of exotic gravel and inverted topography at Crooked Ridge, northern Arizona: Relicts of an ancient river of regional extent: *Geosphere*, v. 16, p. 533-545.

MacCarthy, J. K., Aster, R.C., Dueker, K., Hansen, S., Schmandt, B., and Karlstrom, K., 2014, Seismic tomography of the Colorado Rocky Mountains upper mantle from CREST: Lithosphere–asthenosphere interactions and mantle support of topography: *Earth Planetary Sciences Letter*, v. 402, p. 107– 119.

Macklin, M.G., Fuller, I.C., Lewin, J., Maas, G.S., Passmore, D.G., Rose, J., Woodward, J.C., Black, S., Hamlin, R.H.B., Rowan, J.S., 2002, Correlation of fluvial sequences in the Mediterranean basin over the last 200 ka and their relationship to climate change: *Quaternary Science Reviews*, v. 21, p. 1633-1641.

Maddy, D., Bridgland, D.R., Green, C.P., 2000, Crustal uplift in southern England: evidence from the river terrace records: *Geomorphology*, v. 33, p. 167–181.

Marchetti, D.W., Cerling, T.E., 2005, Cosmogenic ^3He ages of Pleistocene debris flows and desert pavements in Capital Reef National Park, Utah: *Geomorphology*, v. 67, p. 423–435

Mark, D.F., Renne, P.R., Dymock, R.C., Smith, V.C., Simon, J.I., Morgan, L.E., Staff, R.A., Ellis, B.S., Pearce, J.G., 2017, High-precision $^{40}\text{Ar}/^{39}\text{Ar}$ dating of Pleistocene tuffs and temporal anchoring of the Matuyama-Brunhes boundary: *Quaternary Geology*, v. 39, p. 1-23.

Mathews, N.E., Vazquez, J.A., Calvert, A.T., 2015, Age of the Lava Creek supereruption and Magma chamber assembly at Yellowstone based on $^{40}\text{Ar}/^{39}\text{Ar}$ and U-Pb dating of sanidine and zircon crystals: *Geochemistry, Geophysics, Geosystems*, v. 16, p. 2508-2528.

McDougall, I., Harrison, T. M., 1988, *Geochronology and Thermochronology by the $^{40}\text{Ar}/^{39}\text{Ar}$ Method*: New York, Oxford University Press on Demand, 212 p.

McKee, E.D., Wilson, R.F., Breed, W.J., and Breed, C.S., 1967, Evolution of the Colorado River in Arizona: *Museum of Northern Arizona Bulletin*, v. 44, p. 67.

Mckee, E., 2009, The interaction between tectonics, topography, and climate in the San Juan Mountains, Southwestern Colorado [M.S. Thesis] Montana State University, 72 p.

Min, K., Mundil, R., Renne, P. R. and Ludwig, K. R., 2000, A test for systematic errors in $^{40}\text{Ar}/^{39}\text{Ar}$ geochronology through comparison with U–Pb analysis of a 1.1 Ga rhyolite. *Geochim.Cosmochim. Acta* 64, 73–98.

Nereson A.L. Stroud J. Karlstrom K.E. Heizler M.T. McIntosh W., 2013, Dynamic topography of the western Great Plains: Geomorphic and $^{40}\text{Ar}/^{39}\text{Ar}$ evidence for mantle-driven uplift associated with the Jemez lineament of NE New Mexico and SE Colorado: *Geosphere*, v. 9, p. 521-545.

Pederson, J.L., Cragun, W.S., Hidy, A.J., Rittenour, T.M., Gosse, J.C., 2013, Colorado River chronostratigraphy at Lee's Ferry, Arizona, and the Colorado Plateau bull's-eye of incision: *Geology*, v. 41, p. 216-228.

Pelletier, J.D., 2010, Numerical modeling of the late Cenozoic geomorphic evolution of Grand Canyon, Arizona: *Geological Society of America Bulletin*, v. 122, p. 595-608, doi: 10.1130/B26403.1

Polyak, V., Hill, C., and Asmerom, Y., 2008, Age and evolution of the Grand Canyon revealed by U-Pb dating of water table-type speleothems: *Science*, v. 319, p. 1377-1380

Rønnevik, C., Ksienzyk, A.K., Fossen, H., and Jacobs, J., 2017, Thermal evolution and exhumation history of the Uncompahgre Plateau (northeastern Colorado Plateau), based on apatite fission track and (U-Th)-He thermochronology and zircon U-Pb dating: *Geosphere*, v. 13, no. 2, p. 518–537.

Rosenburg, R., Kirby, E., Aslan, A., Karlstrom, K., Heizler, M., Ouimet, W., 2014, Late Miocene erosion and evolution of topography along the western slope of the Colorado Rockies: *Geosphere*, v. 10, p. 641-663.

Sarna-Wojcicki, A.M., Bowman, H.R., Meyer, C.E., Russell, P.C., Woodward, M.J., McCoy, G., Rowe, J.J., Baedeker, P.A., Asaro, F., Michael, H., 1984, Chemical analyses

correlations, and ages of upper Pliocene and Pleistocene ash layers of east-central and southern California: USGS Professional paper, v. 1293, p 46.

Schildgen, T.F., Hodges, K.V., Whipple, K.X., Reiners, P.W., Pringle, M.S., 2007, Uplift of the western margin of the Andean plateau revealed from canyon incision history, southern Peru: *Geology*, v. 35, p. 523-526.

Schmandt, B. and Humphreys, E., 2010, Seismic heterogeneity and small-scale convection in the southern California upper mantle: *Geochemistry, Geophysics, Geosystems*, v. 11, p. 1-19.

Strahler, A.N., 1948, Geomorphology and structure of the west Kaibab fault zone and Kaibab Plateau, Arizona: *Geological Society of America Bulletin*, v. 59, p. 513-540.

van den Berg, M.W., and van Hoof, T., 2001, The Maas terrace sequence at Maastricht, SE Netherlands: evidence for 200 m of late Neogene and Quaternary surface uplift: *River Basin Sediment Systems: Archives of Environmental Change*, Balkema, Abingdon, England, p. 45-86.

Walk, C.J., Karstrom., K.E., Crow, R.S., Heizler, M.T., 2019, Birth and evolution of the Virgin River fluvial system: ~1 km of post-5 Ma uplift of the western Colorado Plateau: *Geosphere*, v. 15, p. 759-782.

Westaway, R., 2001, Flow in the lower continental crust as a mechanism for the Quaternary uplift of Rhenish Massif, northwest Europe: *River Basin Sediment Systems: Archives of Environmental Change*, Balkema, Abingdon, England, p. 87-167.

Westaway, R., 2002, Long-term river terrace sequences: evidence for global increases in surface uplift rates in the late Pliocene and early Middle Pleistocene caused by flow in the lower continental crust induced by surface processes: *Netherlands Journal of Geosciences*, V. 81, p. 305-328.

Westaway, R., Bridgland, D.R., Sinha, R., Demir, T., 2009, Fluvial sequences as evidence for landscape and climatic evolution in the Late Cenozoic: A synthesis of data from IGCP 518: *Global and Planetary Change*, v. 68, p. 237-253.

Willis, G.C., 2004, Interim geologic map of the lower San Juan River area, eastern Glen Canyon National Recreation Area and vicinity, San Juan County, Utah: Utah Geological Survey Open-File Report 443DM (GIS data), 20 p., scale 1:50,000.

Wolkowinsky, A.J., Granger, D.E., 2004, Early Pleistocene incision of the San Juan River, dated with ^{26}Al and ^{10}Be : *Geology*, v. 32, p. 749-752.

York, D., Hall, C.M., Yanase, Y., Hanes, J.A., Kenyon, J., 1981, $^{40}\text{Ar}/^{39}\text{Ar}$ dating of terrestrial minerals with a continuous laser: *Geophysics Research Letter*, v. 8, p. 1136-1138.